

AD-A042 294

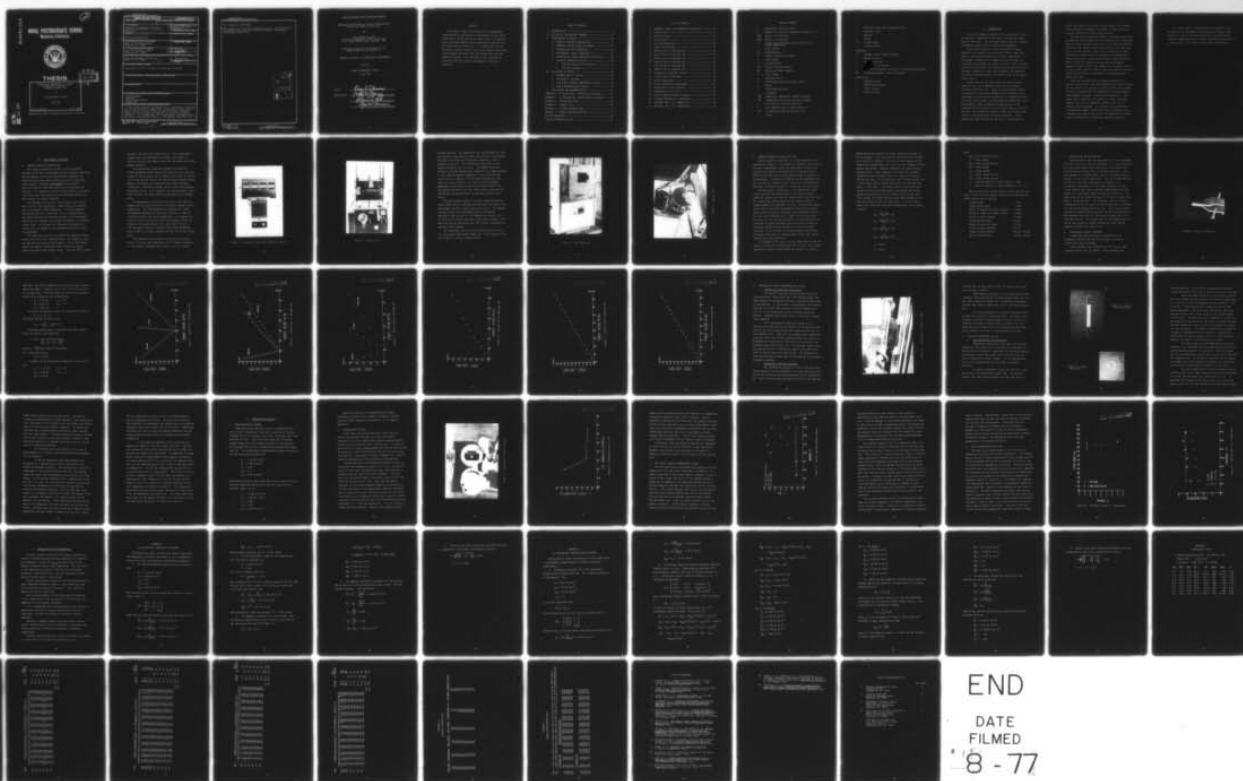
NAVAL POSTGRADUATE SCHOOL MONTEREY CALIF
TEMPERATURE DEPENDENCE OF STRESS CONCENTRATION FACTORS IN COMPO--ETC(U)
JUN 77 R J CHICOINE

F/G 20/11

UNCLASSIFIED

NL

1 of 1
ADA042294



AD A 042294

2

NAVAL POSTGRADUATE SCHOOL

Monterey, California



THESIS

Temperature Dependence of Stress
Concentration Factors In
Composite Materials

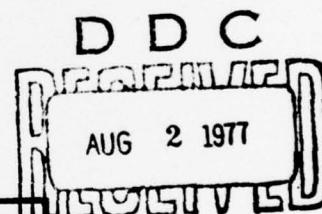
by

Rene Joseph Chicoine

June 1977

Thesis Advisor:

M. H. Bank



AD No. _____
DDC FILE COPY

Approved for public release; distribution unlimited.

UNCLASSIFIED

SECURITY CLASSIFICATION OF THIS PAGE (When Data Entered)

REPORT DOCUMENTATION PAGE		READ INSTRUCTIONS BEFORE COMPLETING FORM
1. REPORT NUMBER	2. GOVT ACCESSION NO.	3. RECIPIENT'S CATALOG NUMBER
4. TITLE (and Subtitle) Temperature Dependence of Stress Concentration Factors in Composite Materials.		5. TYPE OF REPORT & PERIOD COVERED Master's Thesis, June 1977
7. AUTHOR(s) Rene Joseph/Chicoine		6. PERFORMING ORG. REPORT NUMBER
9. PERFORMING ORGANIZATION NAME AND ADDRESS Naval Postgraduate School Monterey, CA 93940		8. CONTRACT OR GRANT NUMBER(s)
11. CONTROLLING OFFICE NAME AND ADDRESS Naval Postgraduate School Monterey, CA 93940		10. PROGRAM ELEMENT, PROJECT, TASK AREA & WORK UNIT NUMBERS
14. MONITORING AGENCY NAME & ADDRESS (if different from Controlling Office) Naval Postgraduate School Monterey, CA 93940		12. REPORT DATE June 1977
		13. NUMBER OF PAGES 78
		15. SECURITY CLASS. (of this report) UNCLASSIFIED
		15a. DECLASSIFICATION/DOWNGRADING SCHEDULE
16. DISTRIBUTION STATEMENT (of this Report) Approved for public release; distribution unlimited		
17. DISTRIBUTION STATEMENT (of the abstract entered in Block 20, if different from Report)		
18. SUPPLEMENTARY NOTES		
19. KEY WORDS (Continue on reverse side if necessary and identify by block number) Graphite/epoxy Laminate Stress Concentration Temperature		
20. ABSTRACT (Continue on reverse side if necessary and identify by block number) This thesis reports the results of an experimental investigation of the effects of temperature on the strain concentration factor due to a circular hole in a graphite/epoxy laminated composite plate subjected to tension in a principal material direction. It is shown that for the [0/+45/0] laminate tested, the strain concentration factor at 300 degrees Fahrenheit was		

DD FORM 1473
1 JAN 73
(Page 1)EDITION OF 1 NOV 65 IS OBSOLETE
S/N 0102-014-6601

UNCLASSIFIED

SECURITY CLASSIFICATION OF THIS PAGE (When Data Entered)

251 450

1

13

UNCLASSIFIED

SECURITY CLASSIFICATION OF THIS PAGE(When Data Entered)

20. Abstract (continued)

→ 20% greater than the room temperature value. This variation is not predicted by classical solutions based on homogeneous orthotropic elasticity.

REFERENCE for	
AVIS	Yield Section <input checked="" type="checkbox"/>
QTC	Gulf Section <input type="checkbox"/>
UNCLASSIFIED	<input type="checkbox"/>
NOTIFICATION	
BY	
DISTRIBUTION/AVAILABILITY CODES	
Dist.	AVAIL. PRO/OF SPECIAL
A	

UNCLASSIFIED

SECURITY CLASSIFICATION OF THIS PAGE(When Data Entered)

Approved for public release; distribution unlimited

Temperature Dependence of Stress Concentration
Factors in Composite Materials

by

Rene Joseph Chicoine
Lieutenant Commander, United States Navy
B.S., United States Naval Academy, 1967

Submitted in partial fulfillment of the
requirements for the degree of

MASTER OF SCIENCE IN AERONAUTICAL ENGINEERING

from the

NAVAL POSTGRADUATE SCHOOL

June 1977

Author

Rene J. Chicoine

Approved by:

Milton H. Bean Thesis Advisor

Richard W. Bell
Chairman, Department of Aeronautics

Robert R. Dorman
Dean of Science and Engineering

ABSTRACT

This thesis reports the results of an experimental investigation of the effects of temperature on the strain concentration factor due to a circular hole in a graphite/epoxy laminated composite plate subjected to tension in a principal material direction. It is shown that for the $[0/\pm 45/0]_s$ laminate tested, the strain concentration factor at 300 degrees Fahrenheit was 20% greater than the room temperature value. This variation is not predicted by classical solutions based on homogeneous orthotropic elasticity.

TABLE OF CONTENTS

I.	INTRODUCTION -----	9
II.	OUTLINE OF THE RESEARCH PROGRAM -----	12
III.	EXPERIMENTAL PROCEDURE -----	14
	A. COMPOSITE MATERIAL MANUFACTURE -----	14
	B. COMPOSITE MATERIAL QUALITY CONTROL -----	21
	C. SPECIMEN END TAB PREPARATION -----	24
	D. EXPERIMENTAL ELASTIC CONSTANTS -----	24
	E. PHOTOELASTIC STRAIN CONCENTRATION TESTING -----	35
	F. ELEVATED TEMPERATURE TESTING -----	37
	1. Specimen Design and Preparation -----	37
	2. Testing Procedure -----	40
IV.	DISCUSSION OF RESULTS -----	44
	A. SPECIMEN QUALITY CONTROL -----	44
	B. PHOTOELASTIC TESTING -----	45
	C. FLAT PLATE ELEVATED TEMPERATURE TESTING -----	48
	D. STRAIN CONCENTRATION TESTING -----	51
V.	CONCLUSIONS AND RECOMMENDATIONS -----	56
	APPENDIX A - K_T CALCULATION: PHOTOELASTIC SPECIMEN -----	57
	APPENDIX B - K_T CALCULATION: GRAPHITE/EPOXY LAMINATE ----	61
	APPENDIX C - PHOTOELASTIC DATA -----	67
	APPENDIX D - TENSILE TESTS -----	68
	APPENDIX E - ULTIMATE STRENGTH DATA -----	74
	APPENDIX F - STRAIN CONCENTRATION DATA -----	75
	LIST OF REFERENCES -----	76
	INITIAL DISTRIBUTION LIST -----	78

LIST OF FIGURES

1. Automatic Timers and Temperature Controller -----	16
2. Platen Press -----	17
3. Post-Cure Oven -----	19
4. Cut-Off Saw -----	20
5. End Tab Preparation -----	25
6. Riehle Test Machine -----	27
7. Tensile Test of Specimen 200 -----	29
8. Tensile Test of Specimen 245 -----	30
9. Tensile Test of Specimen 290 -----	31
10. Tensile Test of Specimen 104 -----	32
11. Tensile Test of Specimen 105 -----	33
12. Tensile Test of Specimen 201 -----	34
13. Photoelastic Specimen Trimming -----	36
14. Typical Tensile Specimen -----	38
15. Strain Gage Clamp -----	38
16. Stress Concentration Specimens -----	41
17. Photoelastic Stress Patterns -----	46
18. Photoelastic K vs. Y/R -----	47
19. Tensile Specimen Modulus Change -----	49
20. Ultimate Strength vs. Temperature -----	52
21. Specimen 208, K vs. Temperature -----	53
22. Specimen, 305, K vs. Temperature -----	54

TABLE OF SYMBOLS

A	Extensional stiffness matrix
E	Modulus of elasticity, Exponential power of 10
EPSX	Strain in X direction
EPSY	Strain in Y direction
F	Fringe value divided by scale factor (47) of linear compensator
G	Shear modulus
G/E	Graphite/epoxy
K	Strain concentration factor
k	Index number
N	In-plane forces
NN	Normal incidence reading
NO	Oblique incidence reading
n	Total number
Q	Stiffness matrix
\bar{Q}	Transformed reduced stiffness matrix
R	Radius
T	Transformation matrix
t	Thickness
TNN	Temperature correction, normal incidence
TNO	Temperature correction, oblique incidence
X	Axis parallel to force direction
Y	Axis perpendicular to force direction
Y/R	Y distance divided by radius of hole
ϵ	Strain

θ Arbitrary angle from longitudinal axis

ν Poisson's ratio

ρ density

σ Stress

[] A square matrix

{ } A column matrix

Subscript

ij denotes row and column of matrix

s Symmetric matrix

x denotes direction

1 longitudinal direction

2 transverse direction, Two plies (in laminate description)

45 45 degrees between 1 and 2 directions

Superscript

C Composite value

P Photoelastic coating

T Total laminate

0 Middle surface

I. INTRODUCTION

The use of composite materials in construction is not a new concept. Composites of one form or another have been used for centuries. Mud and straw composite bricks, plywood, and Damascus steel are just a few ancient examples.

Unlike metal alloys, in which the various alloyed materials mix together on a microscopic scale, composites preserve the separate identities of their constituents. In microscopic examinations of composite cross-sections the individual constituents are readily visible. With a careful choice of constituents, the composite can be made to exhibit the best properties of each, and frequently the composite will have properties better than those of any of its constituents alone.

Within the past ten years there has been a dramatic growth in the use of advanced composites as aerospace structural materials [1]. These so-called advanced composite materials are made by embedding high-strength and/or high-modulus fibers within an essentially homogeneous matrix. The fibers used in most current production composites, boron and graphite, offer strength-to-weight ratios (in the preferred direction) which are five times those of aluminum or steel, and stiffness-to-weight ratios up to eight times those of the conventional structural materials. These properties, combined with the ability of the designer to

orient the fibers to give high strength where it is needed, without providing unnecessary strength in other directions, give the potential for great weight savings.

The possibility of saving weight in aerospace structures has been the driving factor in the increased use of composites. Weight savings translate immediately into better performance, decreased size, greater range and on-station time, more payload. But the increase in the use of composites has been retarded by uncertainties with respect to the engineering details of its use. Joints and fittings, stress concentrations, effects of lightning strikes and environmental exposure, effects of ballistic impact and low energy impact - all have caused concern. Each of these problems has received attention, and some are considered to be understood well, others less well.

With the increasing use of composite materials in aircraft construction, and the emergence of the VSTOL aircraft and sea control ship concept in naval planning, the problem of stress concentrations in composites at elevated temperatures becomes important. Rapid localized heating of skin panels due to deflected jet exhaust is likely, and where stress risers such as fasteners, cutouts, etc., exist, problems may be expected. In addition, the predictions of a thermal-beam weapon (laser) [2], make it essential that knowledge be gained on the effects of temperature on stress/strain concentrations in advanced composite materials.

As a first step in investigating this problem, it was decided to test specimens of graphite/epoxy laminate under tension at various elevated temperatures to determine the effect of temperature on the strain concentration produced by a central hole. This thesis reports that investigation.

II. OUTLINE OF THE RESEARCH PROGRAM

As an initial investigation of the effect of temperature on strain concentration factors in advanced composite laminates, it was decided to fabricate and test a graphite/epoxy laminate, representative of aircraft skin materials. This material was tested to determine the effects of surface heating on the apparent elastic moduli and the maximum strain concentration factor around a central hole in a tension specimen.

A balanced symmetric layup was chosen to represent a thin composite laminate aircraft skin. The layup chosen was $[0/\pm 45/0]_s$, eight laminae in all, with an overall thickness of .040 inches. The greatest strength and stiffness of this skin is in the zero degree direction, of course, but significant shear and transverse strength are present. Thus this layup is suitable for use in aircraft skin applications.

The first tests conducted were photoelastic evaluations of the location and magnitude of strain concentrations around a central hole in a tensile specimen. These tests gave a good picture of the behavior of the "simulated skin" specimens at room temperature. The full strain field was observable and showed that the strain concentration was in fact greatest at the ends of the diameter perpendicular to the forces. As shown by Lekhnitski [3], only with tension in the principal direction is the stress distribution symmetrical with respect

to both principal directions. When pulled in other directions the stress distribution is symmetric only with respect to the center of the opening and the largest stress is not at the ends of the diameter normal to the acting force. Photoelastic testing ascertained proper strain gage placement for further testing.

Finally, the effect of elevated temperatures on the strain concentration factor at a hole in a tensile specimen was determined by testing specimens at six different temperatures, using strain gages attached to the inner edges of the hole. It was recognized that this placement on the circumference of the hole would introduce relatively minor surface curvature effects in the strain gage data. More important, however, was the fact that it eliminated the necessity of extrapolating the data to the hole, a process which is difficult and tenuous at best, especially since photoelastic testing could not be done at high temperatures and there was a possibility of the strain concentration distribution changing.

III. EXPERIMENTAL PROCEDURE

A. COMPOSITE MATERIAL MANUFACTURE

The composite materials tested in this study were produced in the Naval Postgraduate School Composite Laboratory, the development of which was discussed by Linnander [4]. Graphite/epoxy plates were manufactured in this laboratory from "prepreg" (filaments preimpregnated with matrix material) Rigidite 5208 T300 supplied by Narmco Materials Division. This prepreg is sold in various widths, but twelve inch widths were used and cut to provide enough material to make sixteen inch square laminates.

The prepreg is stored in a freezer due to its limited shelf life at room temperature. Before layup, the prepreg has to be warmed to room temperature. To avoid repeated warming and cooling of the entire roll of prepreg material, the amount required for laminates needed in the foreseeable future was cut, wrapped in wax paper and sealed in individual plastic bags. In this way only the material needed for a single plate was warmed to room temperature when the layup was performed.

The layup tool used was a sixteen inch square by three-eighths of an inch thick aluminum plate. The composite layup for the test was balanced and symmetric, with a zero degree lamina followed by a plus and a minus forty-five degree lamina and another zero degree lamina. This half was mirrored

to make a laminate eight laminae thick. This layup made a laminate that was considerably stronger and stiffer in tension along the zero degree direction than along the ninety degree direction.

The laminate was sandwiched between two sheets of TX1040 permeable teflon coated glass separator ply, and nine layers of 120 dry glass fabric bleeder plies (four on top and five on the bottom) to give the desired graphite/epoxy volume percent, followed by the aluminum plates which had been coated with a "Ram-Part" release agent to facilitate separation after curing. This "sandwich" was then wrapped in mylar film to retain any excess epoxy not absorbed by the bleeder plies.

A thermocouple was placed in the edge of the laminate between the mid layers to monitor the actual laminate curing temperature. This thermocouple was connected to a Leeds and Northrup Speedomax-H strip chart recorder in order to record and control the curing temperature. To automate the timing of the curing cycle, series 325 automatic timers by Automatic Timing and Controls Inc. were used (Figure 1). A 50 ton Wabash Hydraulic (platen) Press model 50-45M was used (Figure 2) to apply pressure and heat during the curing cycle.

The temperature and pressure cure cycle used was an initial rise from room temperature to 275 degrees Fahrenheit at five degrees Fahrenheit per minute, with only contact

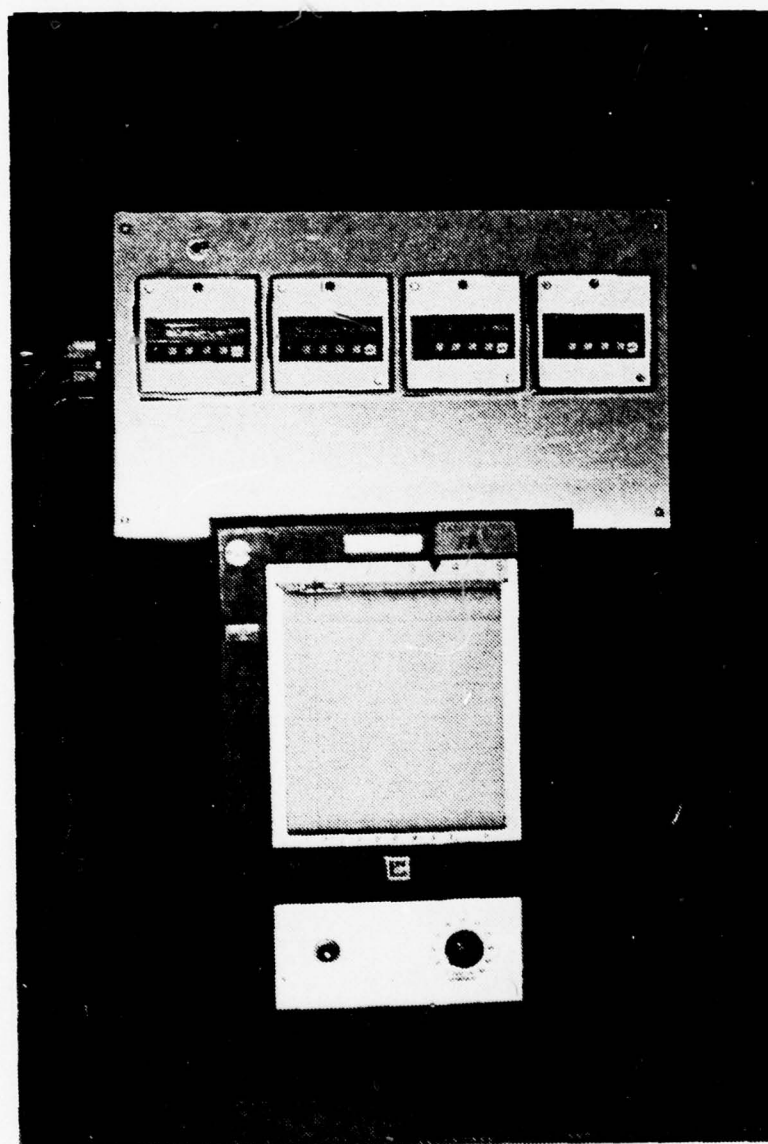


Figure 1. Automatic Timers and Temperature Control

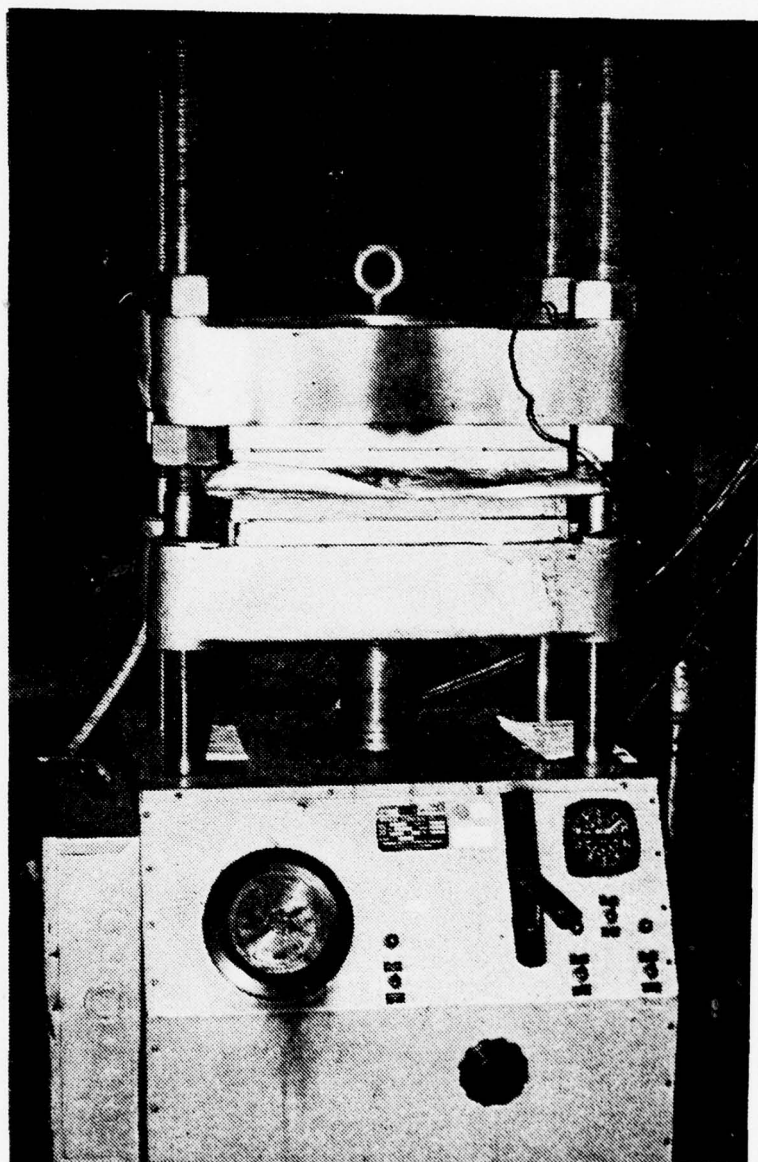


Figure 2. Platen Press

pressure applied. The temperature was held constant at 276°F for one hour, after which it again was raised at five degrees Fahrenheit per minute to 355 degrees Fahrenheit, under a pressure of 80 psig. The laminate was then cured at 355 degrees Fahrenheit for two hours. The heaters were then turned off and the laminate was allowed to cool under pressure to less than 140 degrees Fahrenheit. After removing the plate from the "sandwich," the finished laminate was post cured in a Blue M Electric Co. model CW-7712G automatic temperature controlled air-circulating oven (Figure 3) at 400 degrees Fahrenheit for four hours, after a slow rise to temperatures of approximately two degrees Fahrenheit per minute.

Fiberglass/epoxy plates of Scotchply Brand Reinforced Plastic type 1003 for specimen end tabs were also made in the same manner but with a simplified curing cycle. The temperature was raised from room temperature to 330 degrees Fahrenheit under 80 psig at five degrees per minute, held for thirty-five minutes and then cooled under pressure. The layup for the end tab plates was nine laminae, alternated at zero and ninety degrees.

The plates were cut out to the required specimen size on a Felker-Bay State-Dresser Model 41A liquid cooled cut off saw (Figure 4), using a diamond blade.

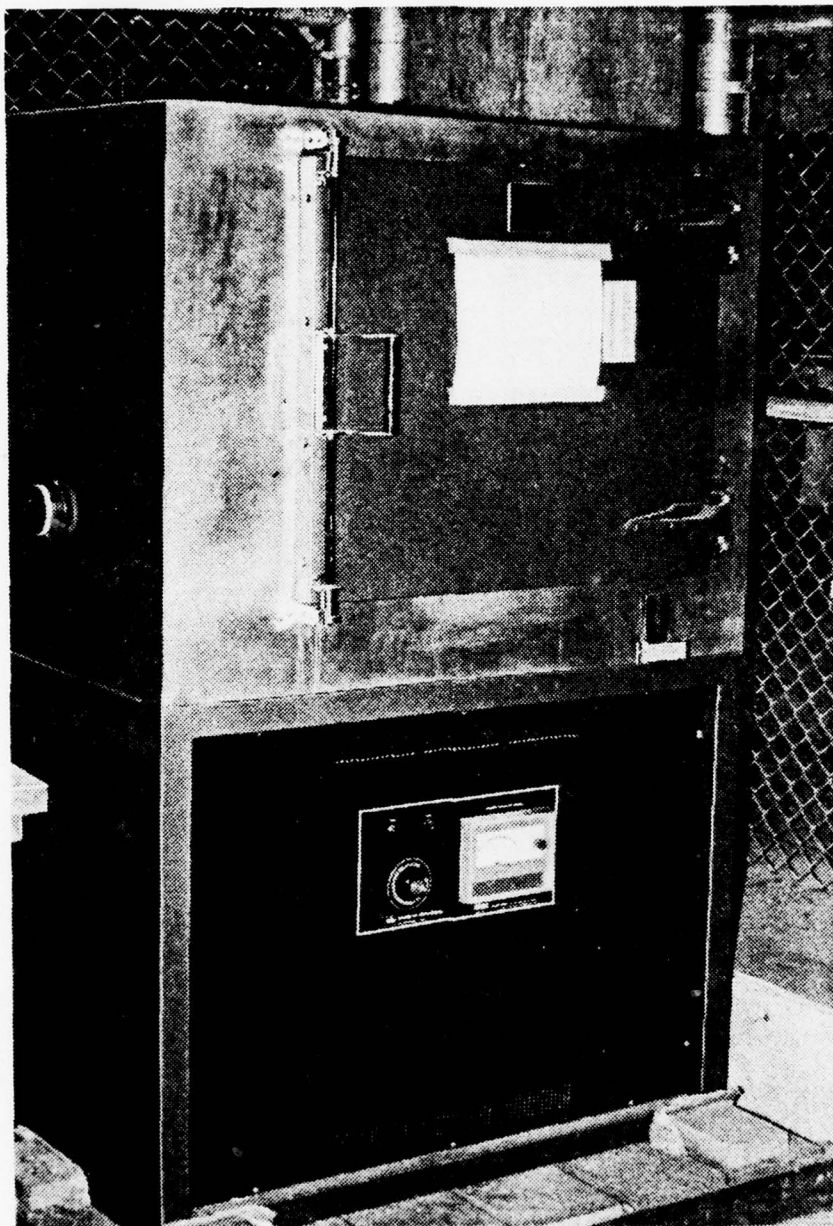


Figure 3. Post-Cure Oven

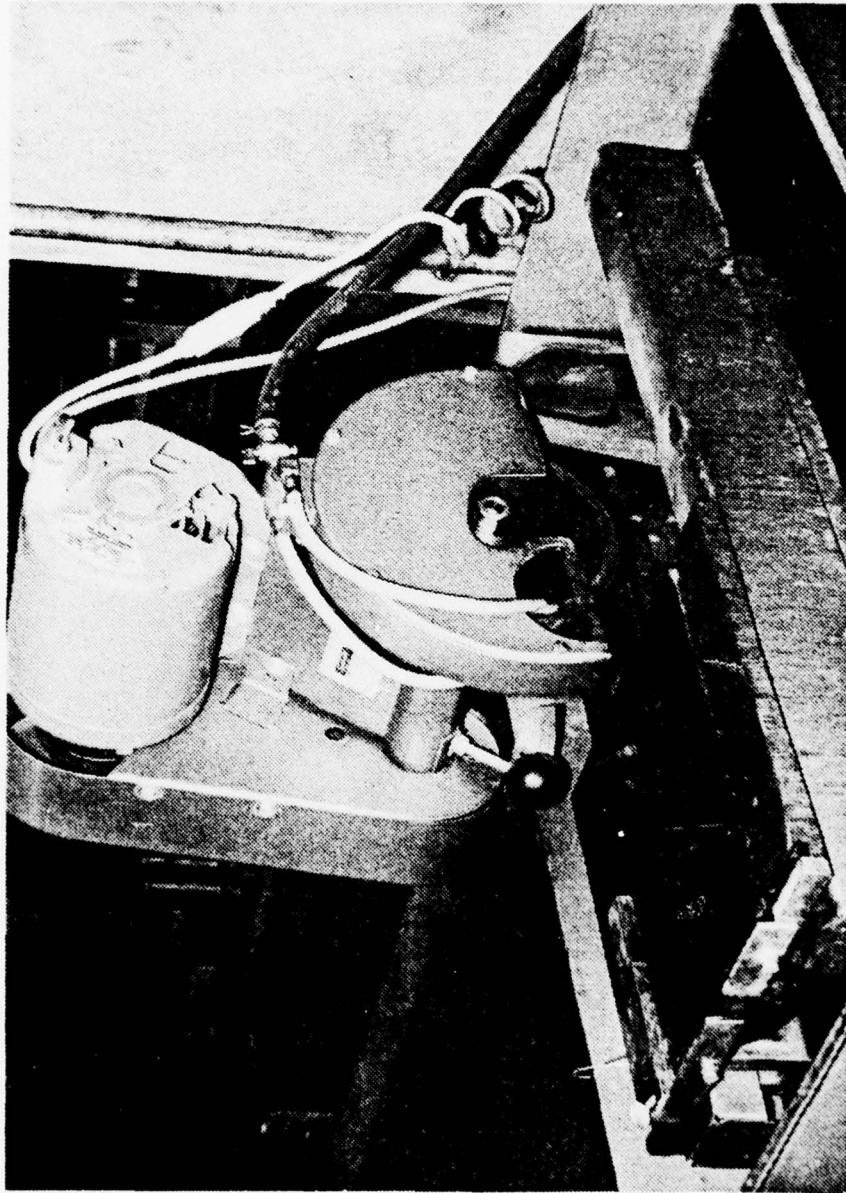


Figure 4. Cut-Off Saw.

B. COMPOSITE MATERIAL QUALITY CONTROL

Quality control of specimens is a major concern in any experimental endeavor. The composites laboratory facility at the Naval Postgraduate School was developed to ensure that high quality composite specimens could be manufactured by different personnel with no noticeable change in quality of the specimens. Linnander [4] reported on the development of this lab and its automatic cycle timers and time/temperature recorders, pictured in Figure 1, to monitor the cure cycle.

Besides careful manufacture, as an added check, fiber volume fractions were determined by the "Hot Acid Resin Digestion" method which was outlined by Hanley and Cross [5]. This method was chosen because of the relative ease of accomplishment with favorable results. Previous work done by Ferris [6] at the Naval Postgraduate School using standard quantitative microscopy techniques gave comparable results to hot acid resin digestion for a coupon from the same plate. This work in turn verified the work of Cilley, Roylance, and Schneider [7] which concluded that the hot acid digestion technique, despite the uncertainties of the constituent densities, is as reliable as the more complex quantitative microscopy techniques if average values rather than spatial distributions are sufficient.

To accomplish this test a coupon, approximately one inch square, was cut on a liquid-cooled cut-off saw. This coupon along with a glass fritted funnel was placed in an oven at

approximately one hundred and eighty degrees Centigrade for thirty minutes. The coupon and the funnel were then weighed on an analytical balance. The resin in the coupon was then digested by concentrated nitric acid that was heated to ninety degrees Centigrade. Complete digestion took approximately twenty minutes. After digestion the fibers were rinsed in Acetone and distilled water until all traces of the resin residue were gone. This liquid was then filtered through the fritted funnel under a vacuum which left only the graphite fibers in the funnel. The funnel and the fibers were then heated in an oven at approximately one hundred and twenty degrees Centigrade for two and one-half hours to dry them. After drying, the fibers and the funnel were weighed on the same analytical balance used previously. From this data, weight and volume fractions were computed with the following formulas:

$$W_{r\%} = \frac{W_s - W_f}{W_s} \times 100$$

$$W_{f\%} = \frac{W_s - W_r}{W_s} \times 100$$

$$V_{r\%} = \frac{V_r}{V_f + V_r} \times 100$$

$$V_{f\%} = \frac{V_f}{V_f + V_r} \times 100$$

$$V_r = W_r / \rho_r$$

$$V_f = W_f / \rho_f$$

where:

$W_{r\%}$ = resin weight fraction

W_r = resin weight

$W_{f\%}$ = fiber weight fraction

W_f = fiber weight

W_s = coupon weight

$V_{r\%}$ = resin volume fraction

$V_{f\%}$ = fiber volume fraction

ρ_r = specific density of resin (epoxy = 1.265)

ρ_f = specific density of fiber (graphite = 1.9 - 2.3)

Resin digestion of sample coupons yielded results very close to the sixty five percent graphite by volume desired.

Sample results are as follows:

Coupon number	200
Coupon weight (gms)	1.0285
Weight of coupon and funnel (before)	13.8190
Weight of fibers and funnel (after)	13.5698
Weight of epoxy (grams)	0.2492
Weight percent epoxy	24.23%
Weight of graphite (grams)	0.7793
Weight percent graphite	75.77%
Graphite volume percent	63.23% - 67.55%
Epoxy volume percent	32.45% - 36.77%

C. SPECIMEN END TAB PREPARATION

Fiberglass/epoxy end tabs were used on all test specimens. They were laid up as cross-ply laminates, i.e., in alternating zero and ninety degree fiber directions, nine lamina thick with the top and bottom plies in the zero direction. They were tapered to a fifteen degree angle in the zero direction giving a "chisel point" appearance. This was accomplished by placing the four pads to be used on a specimen in a "Jorgensen" clamp spaced at the proper intervals to give a fifteen degree taper angle, and then sanding them on a belt sander until the proper taper was achieved (Figure 5). This taper provided for smooth introduction of load into the test section of the specimen. The individual lamina were seven-thousandths of an inch thick, giving the end tabs a thickness of sixty-three-thousandths of an inch. After light surface sanding and degreasing with Acetone the tabs were attached to the specimens with APCO 210 low viscosity epoxy resin with APCO 180 catalyst. This epoxy cures at room temperature, or can be oven cured for greater strength at three hundred degrees Fahrenheit for eight hours.

D. EXPERIMENTAL ELASTIC CONSTANTS

To determine the constitutive properties of the $[0/\pm 45/0]_5$ laminate that was being tested, a series of tensile tests were performed.

Three specimens were prepared with SR-4 strain gage rosettes located near the center. These rosettes were

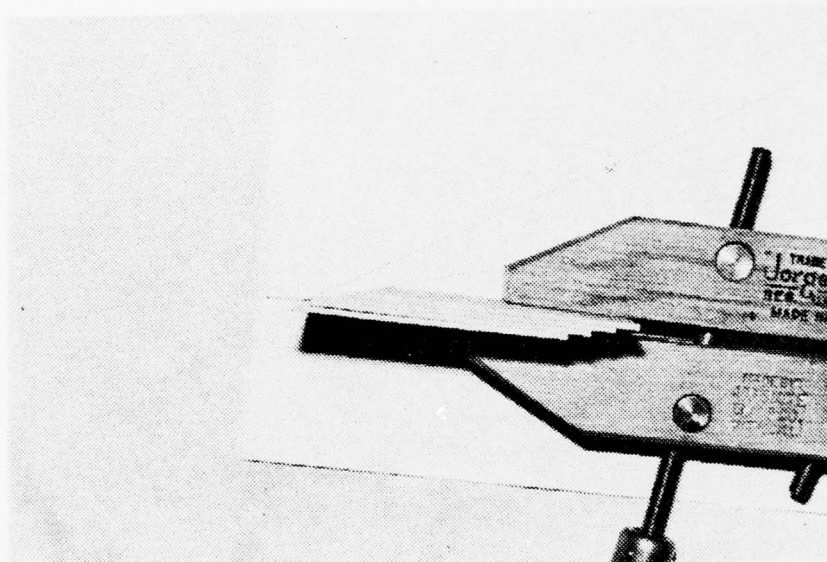


Figure 5. End Tab Preparation.

FABR-24-12 type with a 120 ohm resistance and a 2.04 gage factor. Three other specimens were prepared with a single C9-141 gage with a 350 ohm resistance and a 2.07 gage factor manufactured by the Budd Company. These gages were wired into a Wheatstone bridge circuit with an adjustable power supply and calibrated to read one micro-volt per micro-strain.

The specimens were prepared as basically outlined in the Advanced Composites Design Guide [8]. Specimens numbered 200, 201, 104, and 105 were cut with their lengths parallel to the zero direction fibers. Specimen number 290 was cut with its length ninety degrees to the zero direction fibers. Specimen number 245 was cut with its length forty-five degrees to the zero fibers (or parallel to the two forty-five degree fibers). These specimens were cut into one inch widths, ten-and-one-half inches long. Fiberglass/ epoxy end tabs consisting of nine laminae of alternating zero and ninety degree fiber directions were epoxied to both sides of the specimens as described earlier. These tabs were one inch wide, two-and-one-quarter inches long, and beveled at fifteen degrees to evenly distribute the stresses into the specimen while protecting the graphite/epoxy from being crushed or "broomed" by the test grips. The overall specimen length was ten-and-one-half inches, with a six inch test section length between the fiberglass/epoxy tabs.

The specimens were mounted in a RIEHLE 300,000 pound universal testing machine, pictured in Figure 6. The

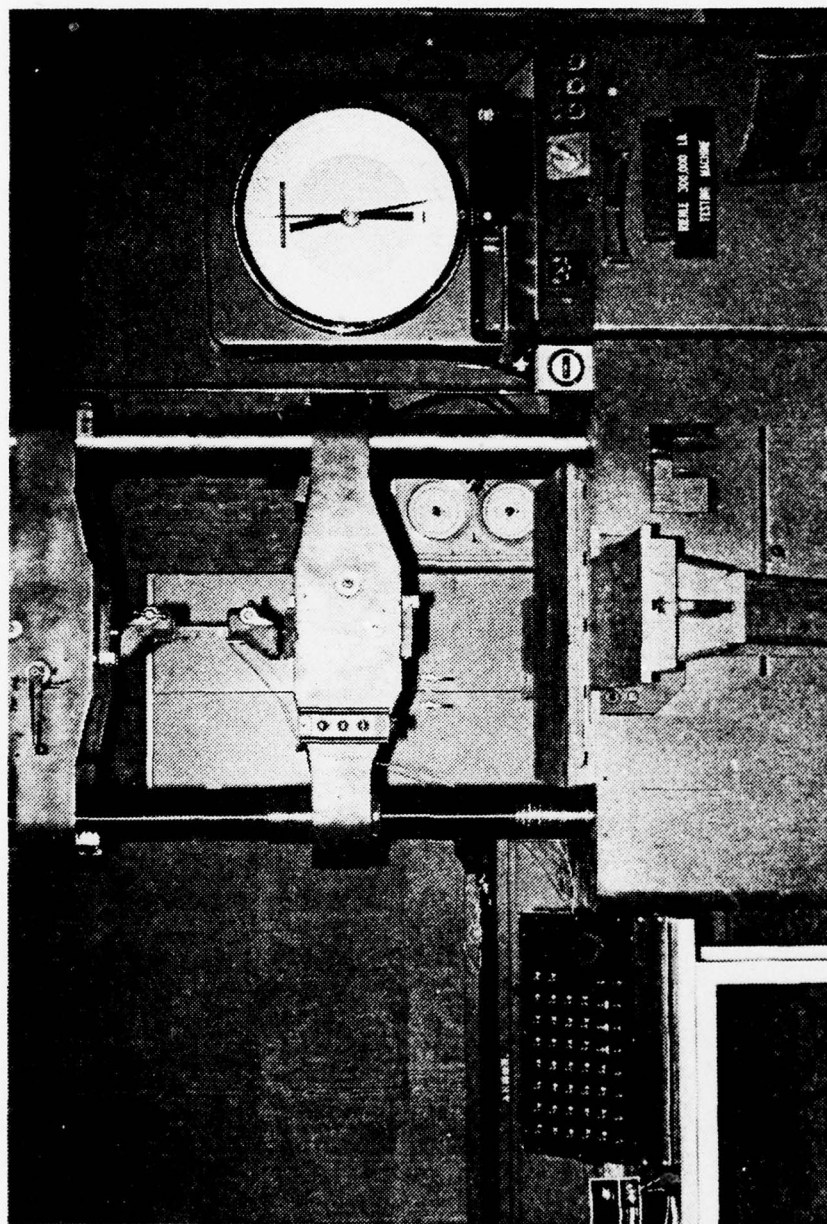


Figure 6. RIEHLE Test Machine.

specimens were slowly loaded to failure while strain measurements were taken. Figures 7, 8, 9, 10, 11 and 12 are plots of the test data. From the graphs the following orthotropic constitutive properties can be determined:

$$E_1 = 11.51 \text{ E6} \quad \nu_{12} = .76$$

$$E_2 = 2.58 \text{ E6} \quad \nu_{21} = .17$$

$$E_x = 6.48 \text{ E6}$$

To verify the Poisson's ratio the "reciprocal relation"

$$E_1 \nu_{21} = E_2 \nu_{12}$$

from Jones [9] can be used giving

$$\nu_{12} = \nu_{21} \frac{E_1}{E_2} = .7584 \approx .76$$

There are several ways to calculate the shear modulus. Using the formula from Jones [9]:

$$G_{12} = \frac{1}{\frac{4}{E_x} - \frac{1}{E_1} - \frac{1}{E_2} + \frac{2\nu_{12}}{E_1}}$$

where $E_x = \frac{P/A}{\epsilon_x}$ when loaded at 45 degrees.

This calculation gives:

$$G_{12} = 3.64 \text{ E6}$$

A summary of the constitutive properties from the tests are:

$$E_1 = 11.51 \text{ E6} \quad \nu_{12} = .76$$

$$E_2 = 2.58 \text{ E6} \quad \nu_{21} = .17$$

$$G_{12} = 3.64 \text{ E6}$$

BEST AVAILABLE COPY

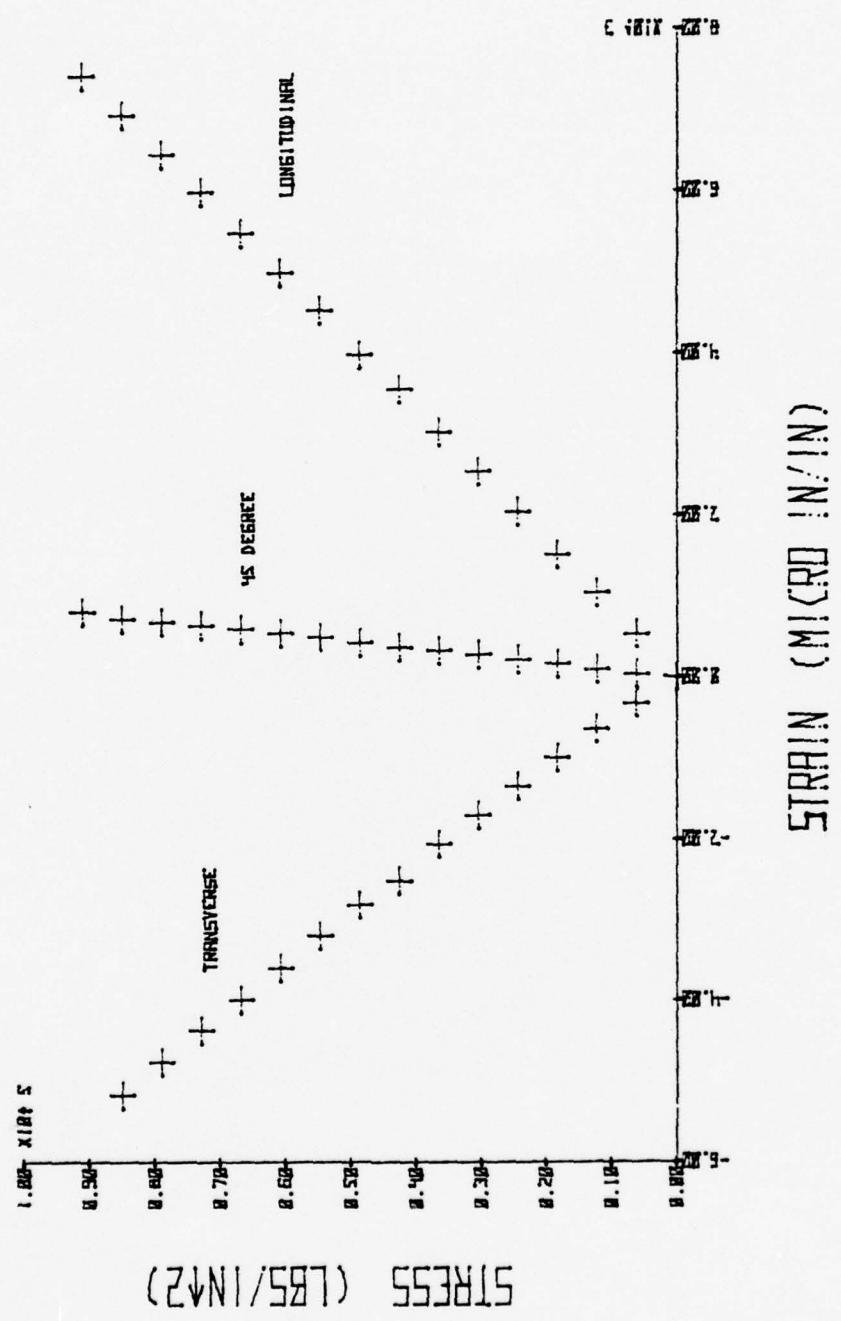


Figure 7. Tensile Test of Specimen 200.

BEST AVAILABLE COPY

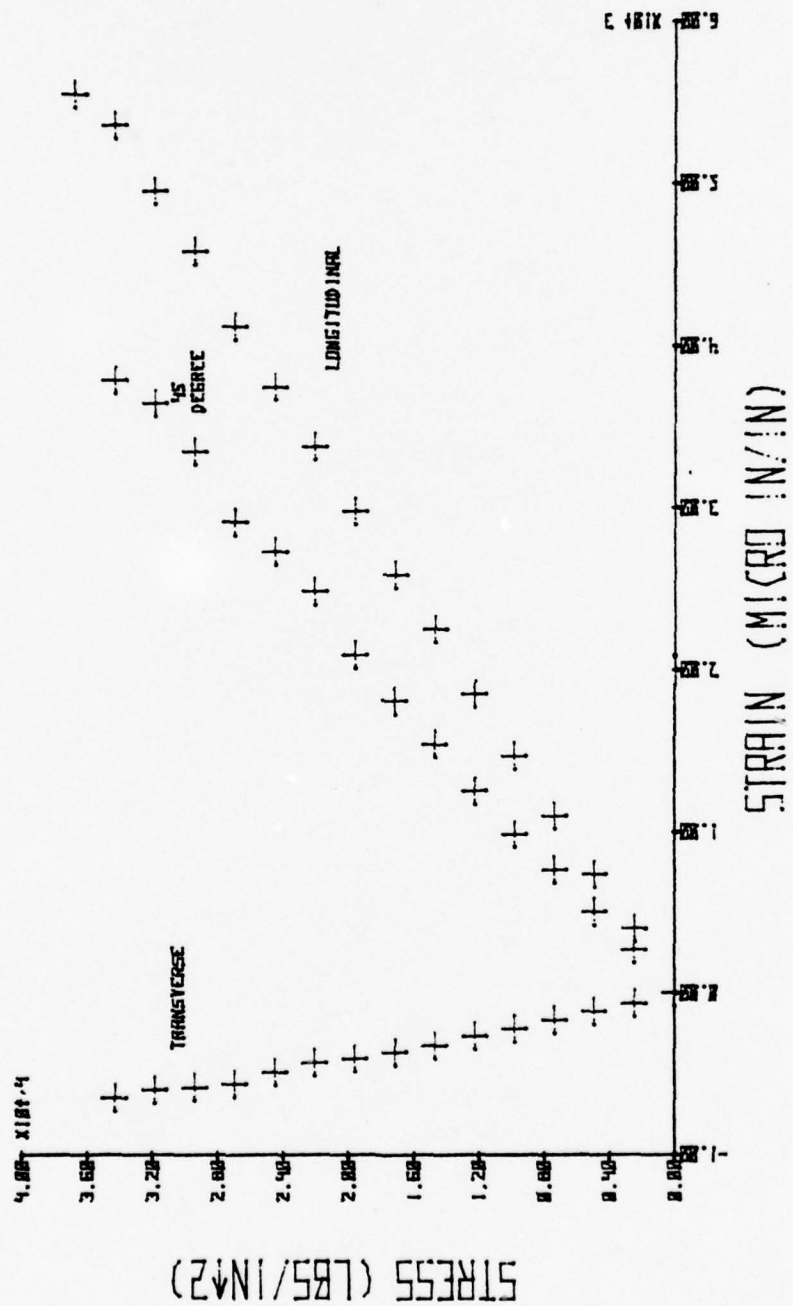


Figure 8. Tensile Test of Specimen 245.

BEST AVAILABLE COPY

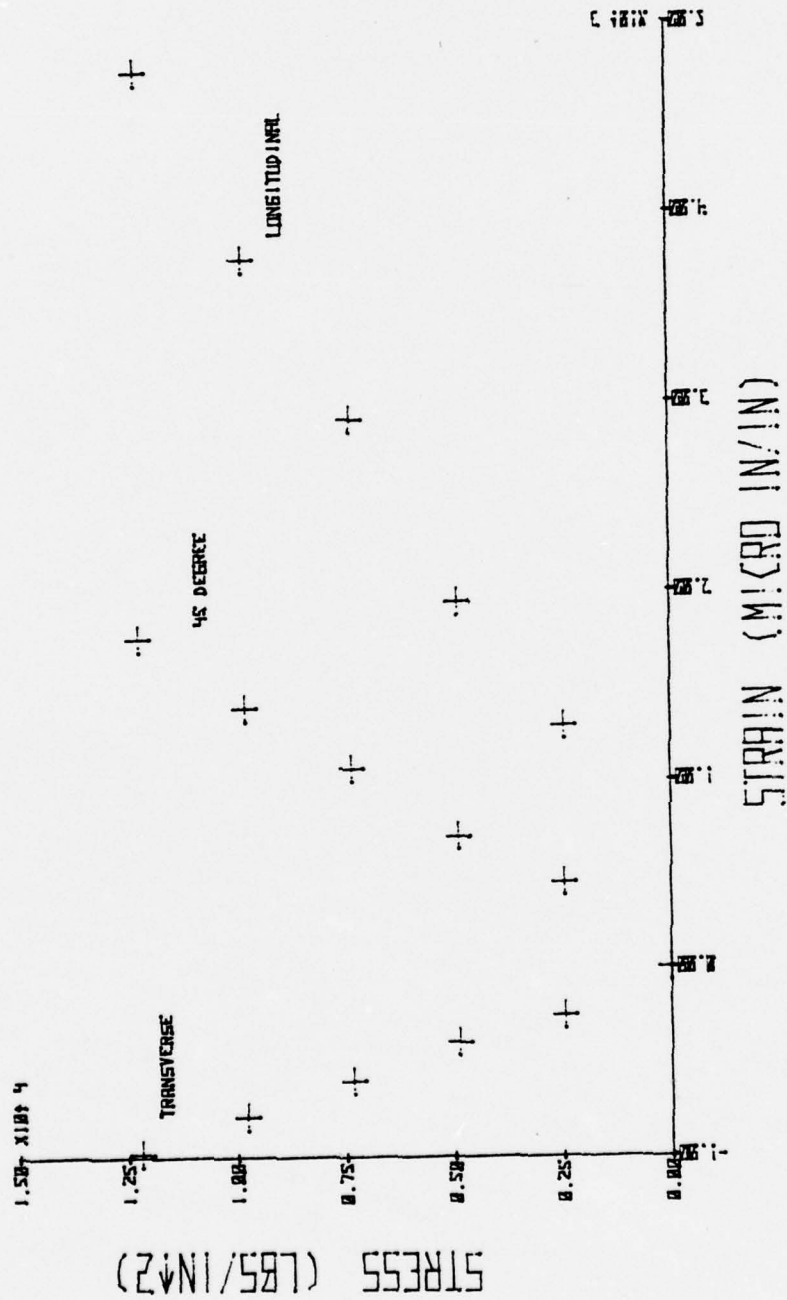


Figure 9. Tensile Test of Specimen 290.

BEST AVAILABLE COPY

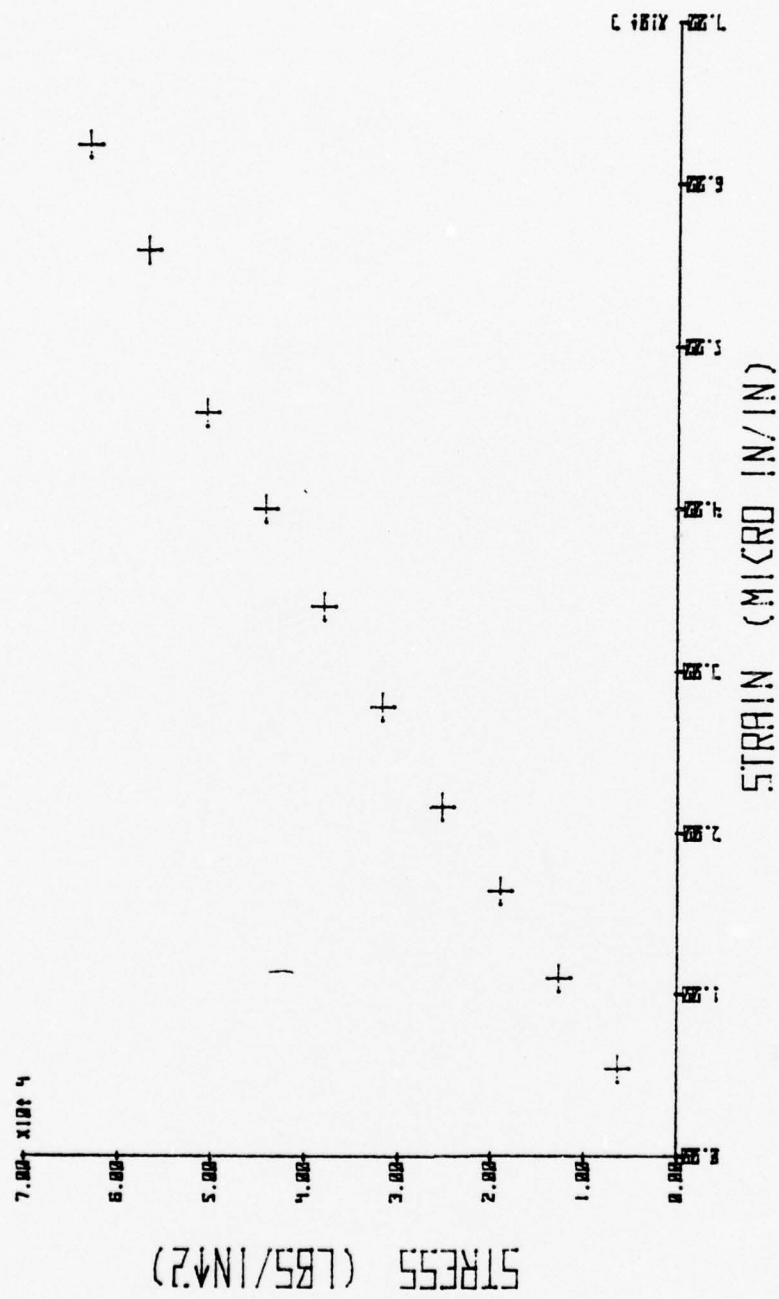


Figure 10. Tensile Test of Specimen 104.

BEST AVAILABLE COPY

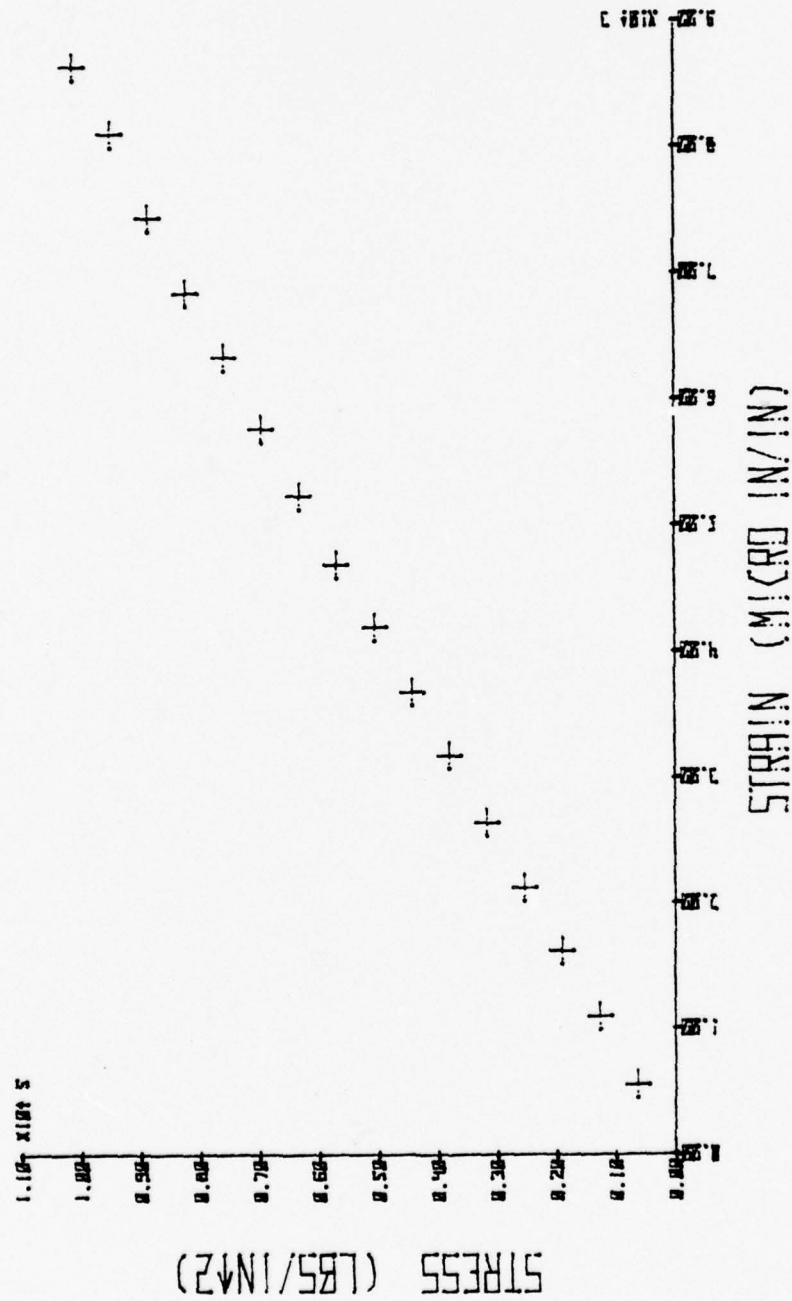


Figure 11. Tensile Test of Specimen 105.

BEST AVAILABLE COPY

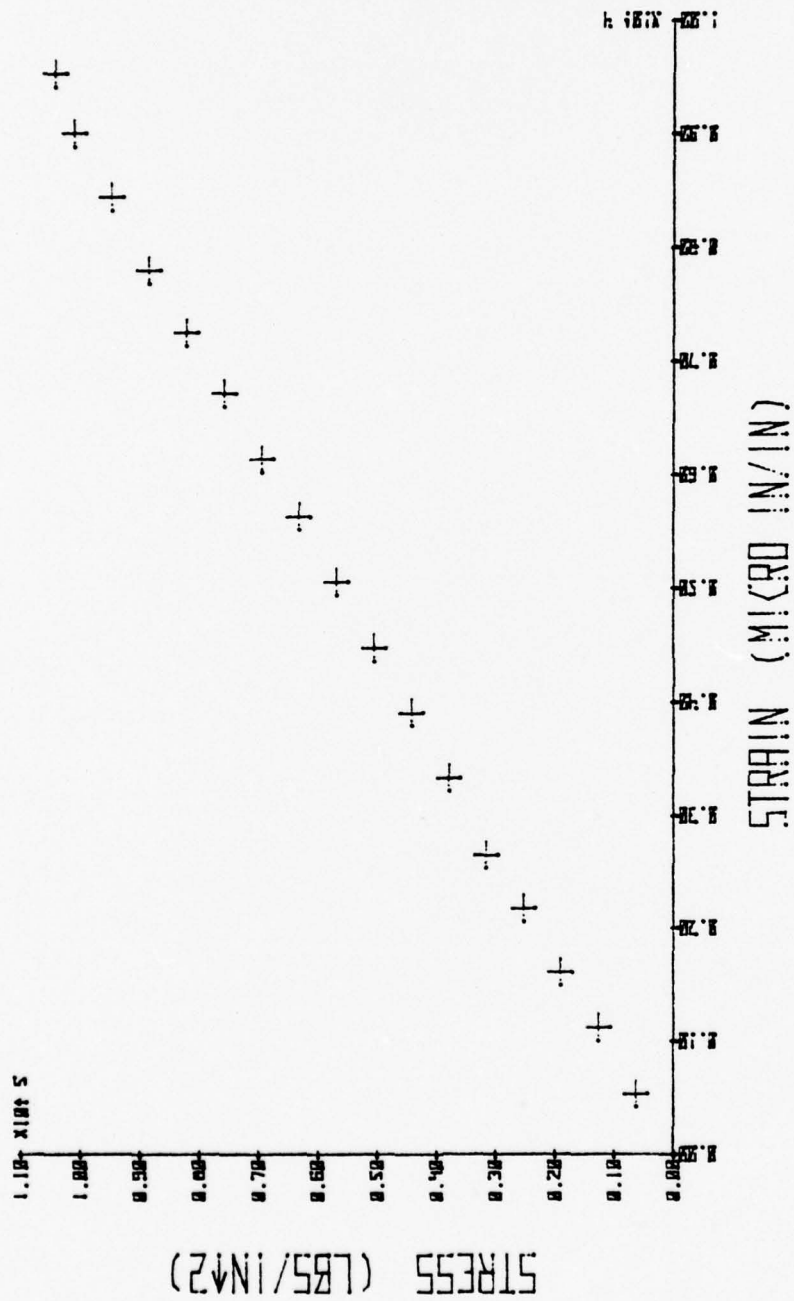


Figure 12. Tensile Test of Specimen 201.

E. PHOTOELASTIC STRAIN CONCENTRATION TESTING

1. Photoelastic Specimen Preparation

The overall specimen size was fifteen inches by two-and-one-half inches with four inch fiberglass/epoxy end tabs, prepared as discussed previously, epoxied on each side of the specimen. In the center a three-quarter inch diameter hole was drilled at 1100 rpm using a Felker diamond core drill in a milling machine with an oil/water spray-mist coolant. Tempered masonite was used as a backing to prevent fiber breakout.

PS-1C photoelastic sheets were glued to the specimen with the sides cut one-eighth inch oversize and the central hole drilled one-eighth inch undersize from the .75 inch diameter hole. After curing the edges were trimmed with a one-half inch, four-fluted high-speed-steel end mill in a Milwaukee milling machine at 195 rpm while cooling with an oil/water spray mist (Figure 13). The hole was reamed using the same machine with a boring bar made of high-speed-tool-steel at 195 rpm using the same coolant. The photoelastic sheet was attached to both sides of the specimen to eliminate unsymmetric bending.

2. Photoelastic Testing Procedure

The specimen was mounted in a Reihle 300,000 pound testing machine and the photoelastic data was taken using the 030 series reflection polariscope manufactured by Photolastic, Inc. Prior to testing the specimen was cycled to the desired

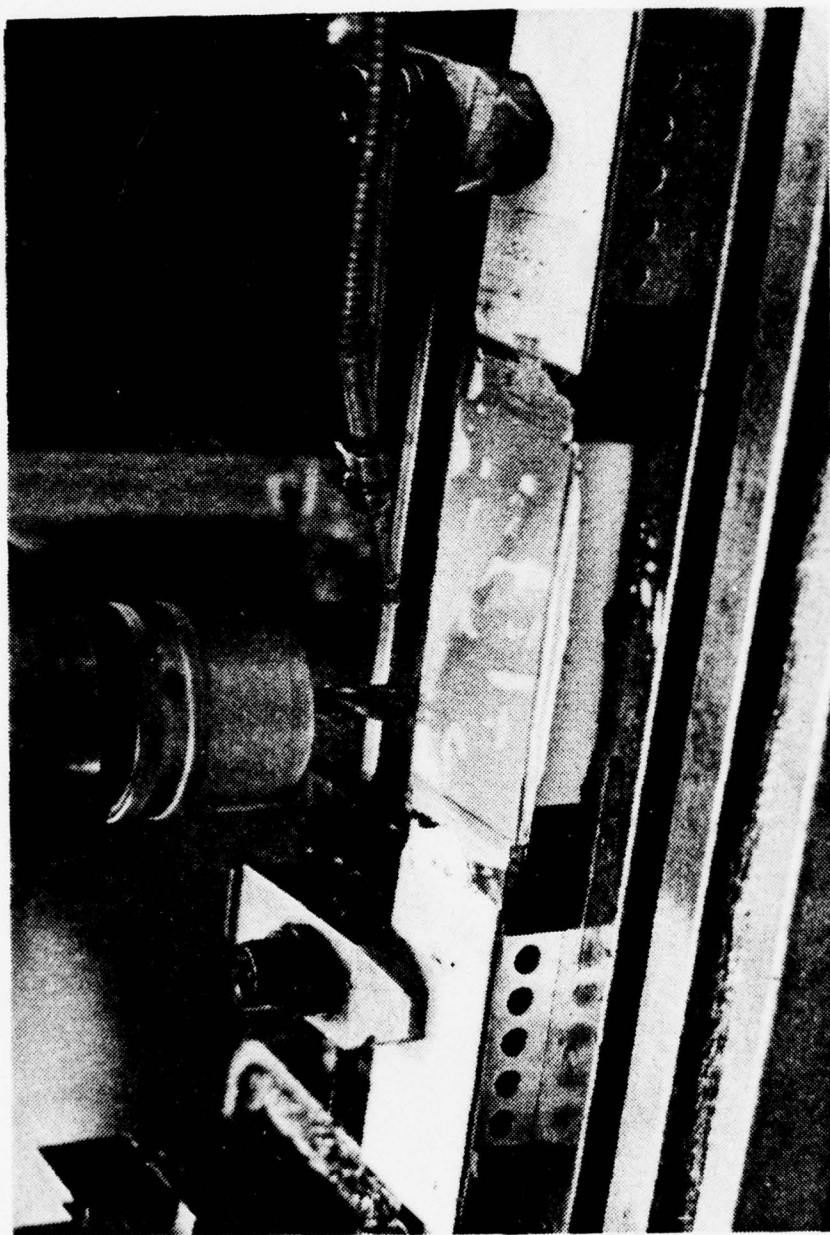


Figure 13. Photoelastic Specimen Trimming.

load and back to zero several times, to reduce scatter due to viscoelastic effects.

Measurements were taken in both normal and oblique incidence, using the oblique incidence adaptor Model 033 and the linear compensator Model 232. Photoelastic procedures used are described in Photolastic, Inc.'s instruction manual [10].

The stress concentration computer program written by Saba [11] was used to reduce the data. The plate in this instance is defined as being loaded in the X-direction and therefore the stress concentrations of interest here are along the Y or unloaded axis. The distance was normalized by the radius of the hole or three-eighths of an inch.

F. ELEVATED TEMPERATURE TESTING

1. Specimen Design and Preparation

Temperature testing was broken down into two main categories: tests that would involve tensile specimens for demonstration of effects of temperature on the major modulus and Poisson's ratio, and plates with a hole for tests of strain concentration factor changes. All of the specimens were cut and loaded along the zero fiber (strongest) direction.

The tensile specimens (Figure 14) were cut in one inch widths, ten-and-one-half inches long. Two-and-one-quarter inch long fiberglass/epoxy end tabs were used as

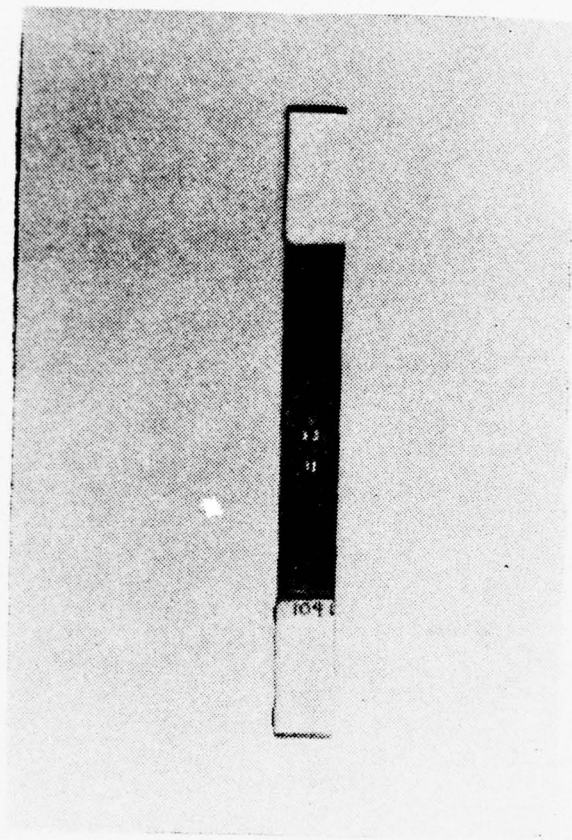


Figure 14. Typical
Tensile Specimen.

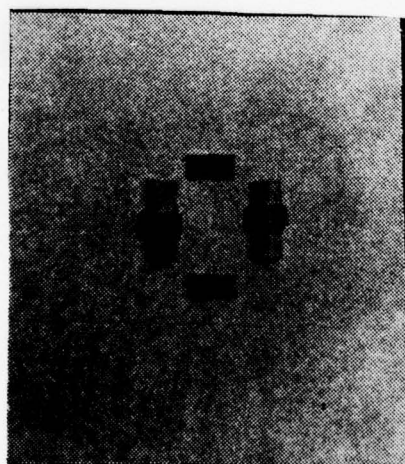


Figure 15. Strain
Gage Clamp.

discussed earlier. On the stress concentration specimens a four-and-one-half inch long by three inch wide tab was used.

One of the major obstacles to the strain concentration test program was the necessity of placing a strain gage in a hole with a .750 inch diameter and a thickness of .040 of an inch. After many trials a method was devised that worked adequately. Figure 15 shows the special clamp that was manufactured from a dowel to apply the pressure needed during curing. The dowel was split lengthwise, a rubber pad was placed over the outside of the dowel to protect the gage, and metal wedges were then used to apply pressure by separating the two halves. The composite surface was prepared for the gage by degreasing with Chloroethene nu, sandblasting lightly with an abrasive powder in a S. S. White Industrial Abrasive Unit Model F, and cleaning with acetone.

The strain gages for room-temperature tests were fastened to the specimens with Micro-Measurements M Bond 200 single-component glue with an activator. The strain gages used in high temperature testing were applied with M Bond 610 two component glue. The M Bond 610 required that the gages be clamped under light pressure and heated via a prescribed heat schedule to 330 degrees Fahrenheit for two hours.

The strain gages used on tensile specimens 106 and 107 were single C9-141 gages manufactured by the Budd Company with a 350 ohm resistance and a gage factor of 2.07. On specimens 204 through 207 and 301 through 304 a three gage rosette (foil C12-121B-R3T) manufactured by the Budd Company,

with a 120 ohm resistance and a gage factor of 2.06, was used. For the specimens with a hole, numbers 208 and 306, Micro-Measurements gages EA-13-031DE-120 were used with a 120 ohm resistance and a gage factor of 2.07.

The stress concentration specimens (Figure 16) were cut fifteen inches long and three inches wide. Four inch long fiberglass/epoxy end tabs were applied as outlined for the tensile specimens.

Temperature sensing was provided with two glass-fabric insulated chromel-alumel thermocouples on the tensile specimens and four thermocouples on the stress concentration samples, placed one inch on either side of the strain gages. These thermocouples were placed on the same side as the strain gages. The specimens were heated on the opposite side by three semi-focused tungsten-filament lamp heaters that were controlled with a variac. They were heated on only one side and the temperature was measured on the opposite side in order to approximate an aircraft skin that was heated with an external energy source from the exterior, while strain and temperature was measured on the interior.

2. Testing Procedure

The specimens were mounted on a 300,000 pound RIEHLE test machine set at a 15,000 pounds maximum scale. The strain gages were connected to a Wheatstone bridge circuit powered by a SRC Division/Moxon Electronics Model 3564

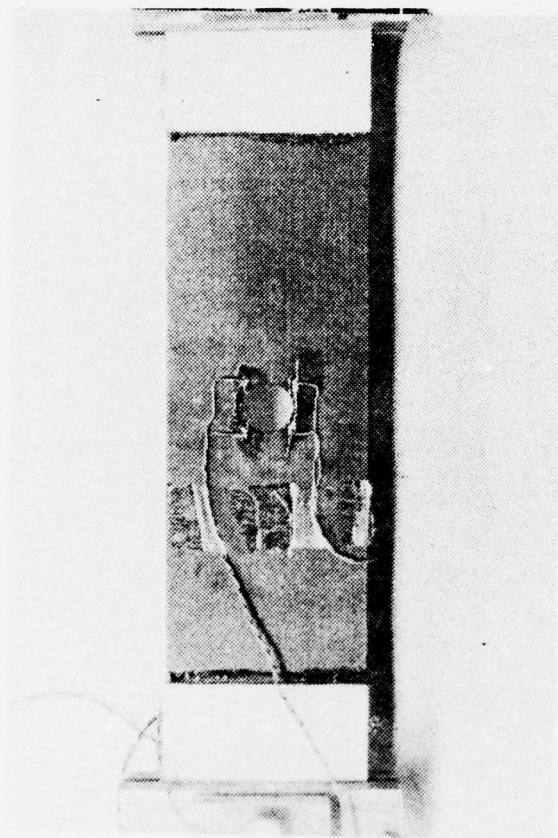


Figure 16. Stress Concentration Specimens.

power supply adjusted to a one amp output. The two-arm bridge was completed by an unused specimen in the compensating leg. The output of the bridge circuit was zeroed and calibrated utilizing a Digitec digital voltmeter. The output was then fed into a Hewlett-Packard 7100B strip chart recorder with an "event marker." The event marker was used to indicate 125 lb load intervals as they were passed, in order to have continuous testing of a specimen while being able to record specific load/strain readings.

To eliminate strain rate effects a slow rate of approximately 4.0 E-5 lb/sec was selected and used throughout the test program.

To monitor temperature the thermocouples were connected via a sealed rotary selector switch to a Doric DS-300 thermocouple indicator. The specimens were heated to temperature in one minute and then held until the reading stabilized (which took approximately three minutes) and then tested. On the tensile specimens where a temperature series was run (i.e., 106, 107, 204, 205, 301 and 302) the specimens were heated incrementally so that when the specimen was tested at 350 degrees Fahrenheit it had by then been "heat soaked" at 150 degrees F for forty minutes, 200 degrees F for thirty minutes, 250 degrees F for twenty minutes and 300 degrees F for ten minutes. These specimens were then cooled down to the temperature for their ultimate failure test and loaded. Specimens 206, 207, 303 and 304 were loaded at room temperature and then heated to temperature and again loaded

for an ultimate failure test to see if prolonged heating made any appreciable difference. On the strain concentration specimens the temperature was brought back to 75 degrees Fahrenheit after each loading run of the series. Temperature uniformity was plus or minus ten degrees Fahrenheit and the average temperature was within five degrees of the nominal temperature.

To eliminate the apparent strain exhibited with temperature change of the strain gages the strain indicator was balanced for zero strain and the test was run after the specimen was temperature stabilized. To compensate for gage factor change Micro-Measurements [12] suggests multiplying the semicorrected strain (i.e., corrected for apparent strain only) by the reference gage factor divided by the gage factor at temperature. For the test temperatures involved this is a maximum change of 1% in gage factor. The surface curvature effects on apparent strain for the gages used mounted in a three-quarter inch diameter hole with "E" backing and 610 adhesive result in a change in incremental apparent strain with temperature of three microinches/°F. This change was eliminated by balancing the strain indicator for zero strain after the temperature was stabilized. The strain gages used were rated for 350 degrees Fahrenheit for continuous use and for 400 degrees Fahrenheit for short term exposure.

IV. DISCUSSION OF RESULTS

A. SPECIMEN QUALITY CONTROL

After manufacture and post cure all laminated plates were visually checked for flaws and indications of residual stresses due to the thermal cure cycle. The plates were flat and free of flaws. "Hot acid resin digestion" of sample coupons showed the fiber volume fractions of the specimens to be between 63% and 67%, bracketing the desired 65% volume fraction. The experimentally determined engineering constants for the laminated specimens were

$$E_1 = 11.51 \text{ E6 lb/in}^2$$

$$E_2 = 2.58 \text{ E6 lb/in}^2$$

$$\nu_{12} = 0.76$$

$$\nu_{21} = 0.17$$

$$G_{12} = 3.64 \text{ E6 lb/in}^2$$

Engineering constants were predicted, based on data from the Advanced Composites Design Guide [8] and using classical laminate theory, to be:

$$E_1 = 12.345 \text{ E6 lb/in}^2$$

$$E_2 = 3.725 \text{ E6 lb/in}^2$$

$$\nu_{12} = 0.669$$

$$\nu_{21} = 0.202$$

$$G_{12} = 3.202 \text{ E6 lb/in}^2$$

Sample calculations for determination of these engineering constants for a symmetric balanced laminate, given the lamina engineering constants, are included in Appendix B.

B. PHOTOELASTIC TESTING

Strain levels at points along the Y-axis (the axis across the specimen, through the center of the hole, perpendicular to the loading direction) were measured photoelastically on a specimen with a central hole. In addition; the strain at a point midway between the hole and the end tabs was measured, giving information on the uniform strain away from the hole. Data taken is shown in Appendix C; Figure 17 shows the photoelastic stress patterns on the specimen.

The maximum strain concentration value at the hole, as calculated from photoelastic data, is $K = 3.22$. As seen in Figure 18 the strain concentration factor drops rapidly as distance from the edge of the hole increases. The axial strain at the outside edge of the plate is only 0.90 of the far-field uniform strain value. When the engineering constants for the graphite/epoxy composite are modified to include the effects of the photoelastic coatings, and then used in Lekhnitshii's [3] classical solution for the stress distribution in an orthotropic plate with a central circular hole under uniaxial tension, the strain concentration factor predicted is $K = 4.08$ (see Appendix B). This is a value 21% higher than that measured. However, the predicted value is

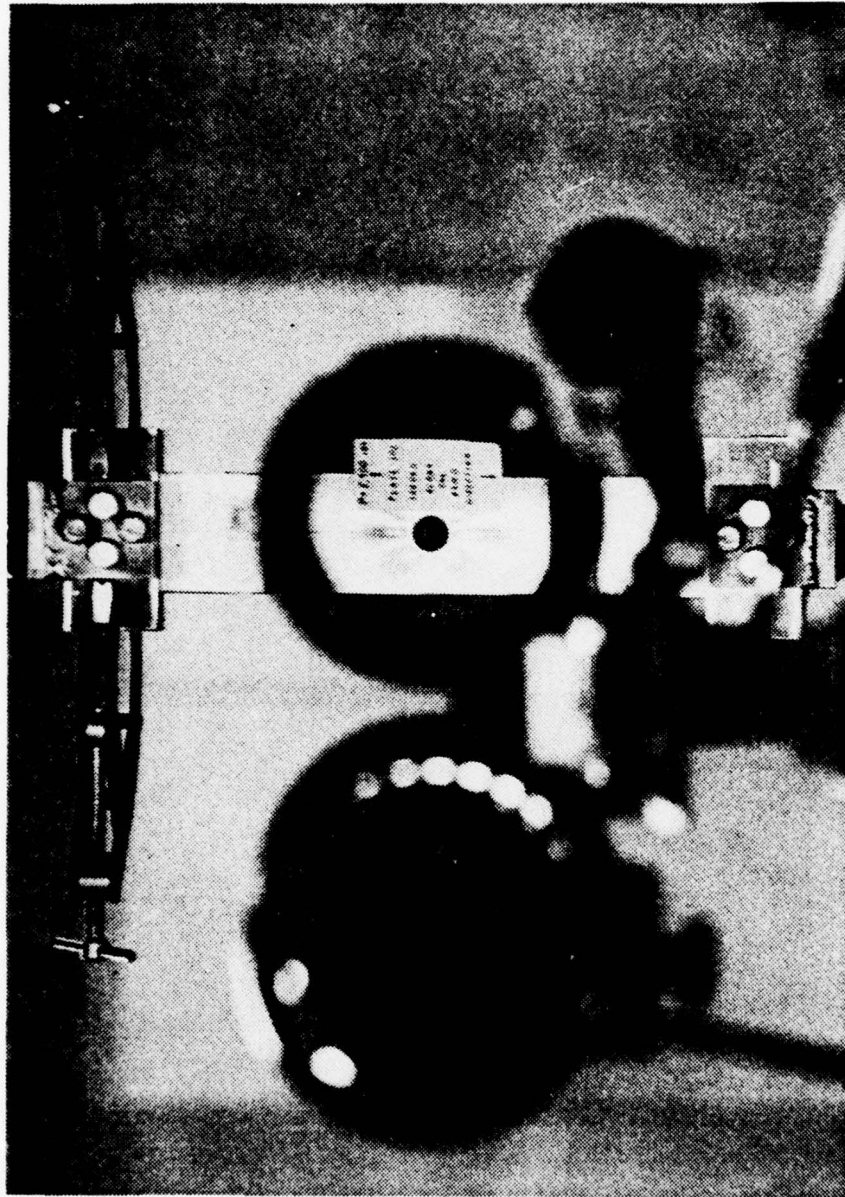


Figure 17. Photoelastic Stress Patterns.

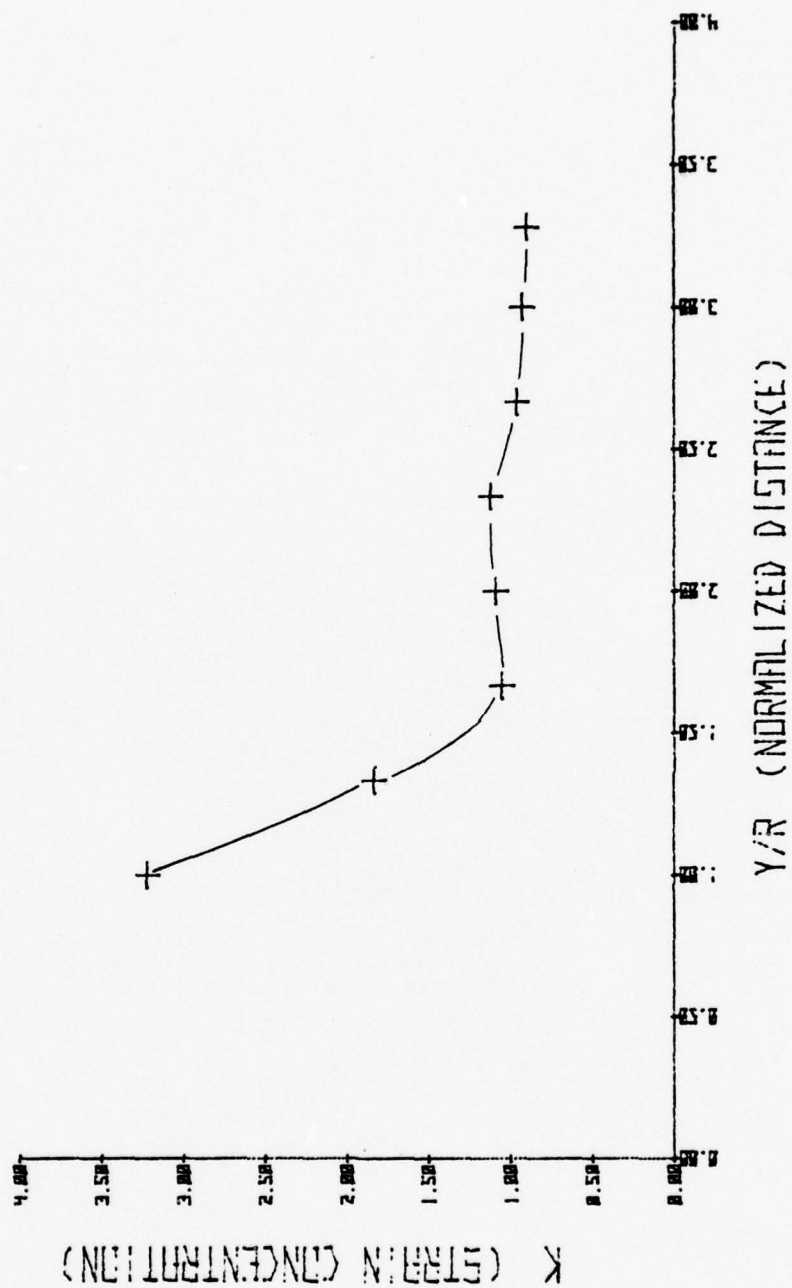


Figure 18. Photoelastic K vs. Y/R.

based on the consideration that the laminate is a homogeneous orthotropic material, rather than a laminate. Daniel, Rowlands and Whiteside [13] found that $[0_2/\pm 45/\bar{0}]_s$ laminates, similar to that used here, have a strain concentration lower than that predicted by homogeneous orthotropic theory, while $[\pm 45/0_2/\bar{0}]_s$ laminates have strain concentration factors greater than the prediction. That is, the strain concentration factor is dependent on the laminate stacking sequence.

As expected, when the composite specimen was subjected to tension along a principal direction of the orthotropic material, the maximum strain occurred at the ends of a diameter of the hole normal to the direction of the applied load.

C. FLAT PLATE ELEVATED TEMPERATURE TESTING

Ten flat plate tensile specimens were tested at varying temperatures with the results tabulated in Appendix D. A graphic depiction of the primary modulus changes is given in Figure 19 which shows the results of an apparent modulus change due to temperature for both heat soaking and short duration heating along with the theoretical results for this laminate. This graph indicates just how far off you can be from the actual average modulus when testing the modulus from one side only on a specimen that was rapidly heated from the other side. There is a good correlation up to 150 degrees Fahrenheit. At 200 degrees Fahrenheit the heat soaked specimens correlate with the predicted values but the

BEST AVAILABLE COPY

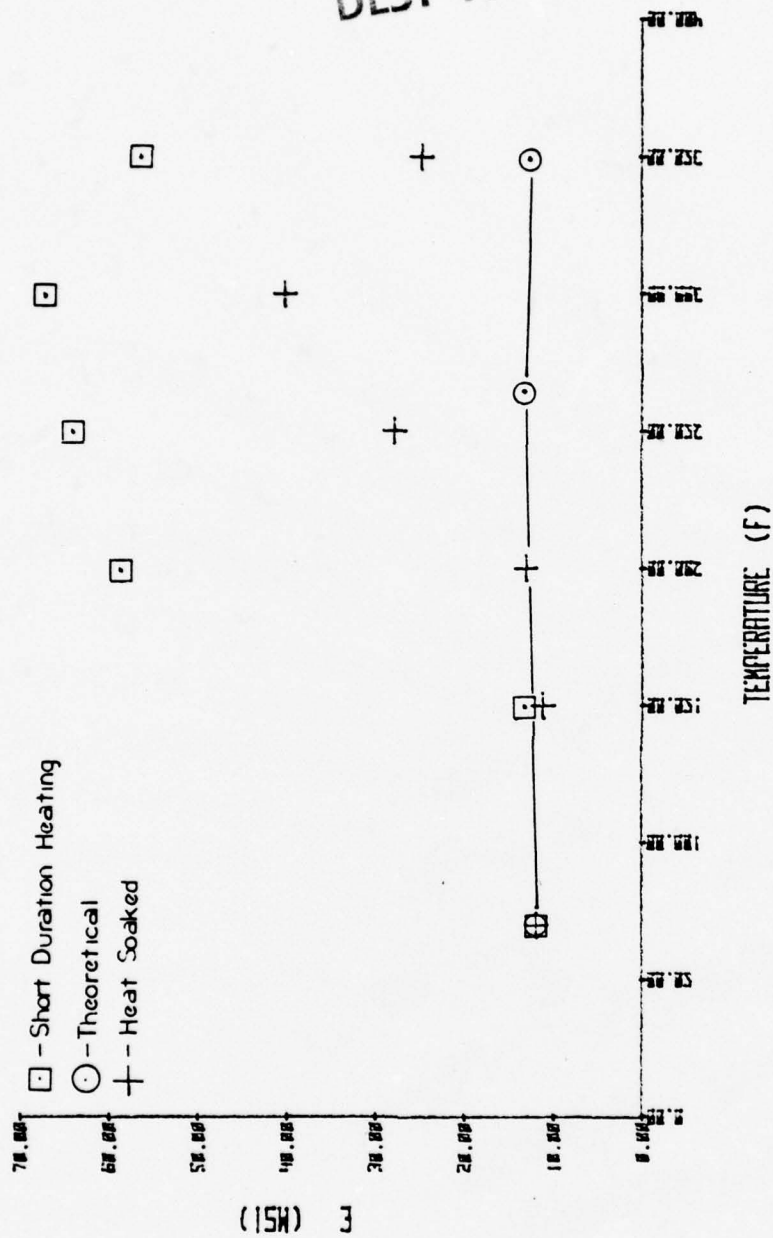


Figure 19. Tensile Specimen Modulus Change.

specimen heated for a short duration has diverged to approximately five times the value of the theoretical solution. From 250 degrees to 350 degrees Fahrenheit the shape of the curve is a highly exaggerated form of the theoretical prediction and for the specimens heated for a short duration the apparent value has diverged from the theoretical value approximately six-fold while for the heat soaked specimens it has diverged approximately three-fold.

This apparent modulus error of a composite plate is of significance in a situation involving heating from one side and measuring of strain values via strain gages on the other side. This situation is possible and even likely if the Navy adopts some type of fatigue life data acquisition for aircraft using microcomputer technology, such as described by Stanfield [14]. With an external heating source the strain recorded on the interior surface of a flat plate appears to be much less than the actual average value of strain carried by the plate. A fatigue life data acquisition system monitoring strain on a composite wing section that is subjected to localized heating due to deflected jet exhaust or other heating source could record the occurrence of significantly less strain than that to which the structure actually was subjected.

The ultimate strengths of the flat plate tensile specimens are listed in Appendix E by number, temperature, heat cycle and type of break. Figure 20 is a graphical display of the ultimate strength versus temperature information shown by

type of heating. Unfortunately, almost half of the specimens tested broke under the end tabs due to problems in introduction of load into the specimens. These data were not included in Figure 20, although they are included in Appendix E. The results in Figure 20 show no discernable pattern due to type of heating and no appreciable ultimate strength variation in the temperature range from room temperature to 350 degrees Fahrenheit.

D. STRAIN CONCENTRATION TESTING

The strain per average stress or net stress at six temperature locations are listed in Appendix F. The average and net values of strain concentration versus temperature for tensile specimens 208 and 305 are plotted in Figures 21 and 22 along with the theoretical prediction. The strain concentration factors were computed by dividing the strain gage data by calculated far-field strain values which were determined by dividing the average or net stress by the temperature-dependent modulus of elasticity. This modulus was computed from experimental data contained in the Advanced Composites Design Guide [8]. Details of the computations are shown in Appendix B. The strain concentration results from the two tensile specimens show a similar pattern and were repeatable. The magnitude variation in the k factor between the specimens was due at least in part to the difficult task of accurate strain gage placement in the hole. The plot of the theoretical values from homogeneous orthotropic material theory

BEST AVAILABLE COPY

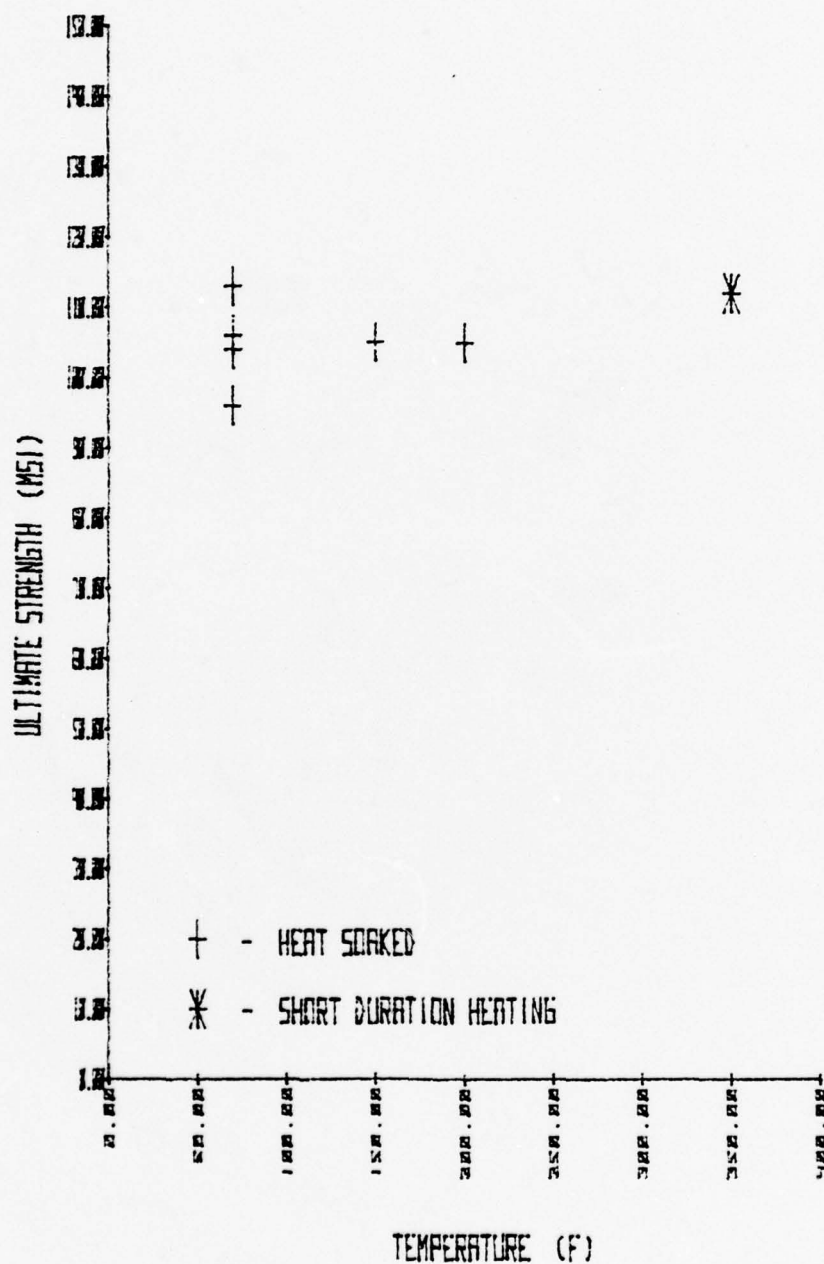


Figure 20. Ultimate Strength vs. Temperature.

BEST AVAILABLE COPY

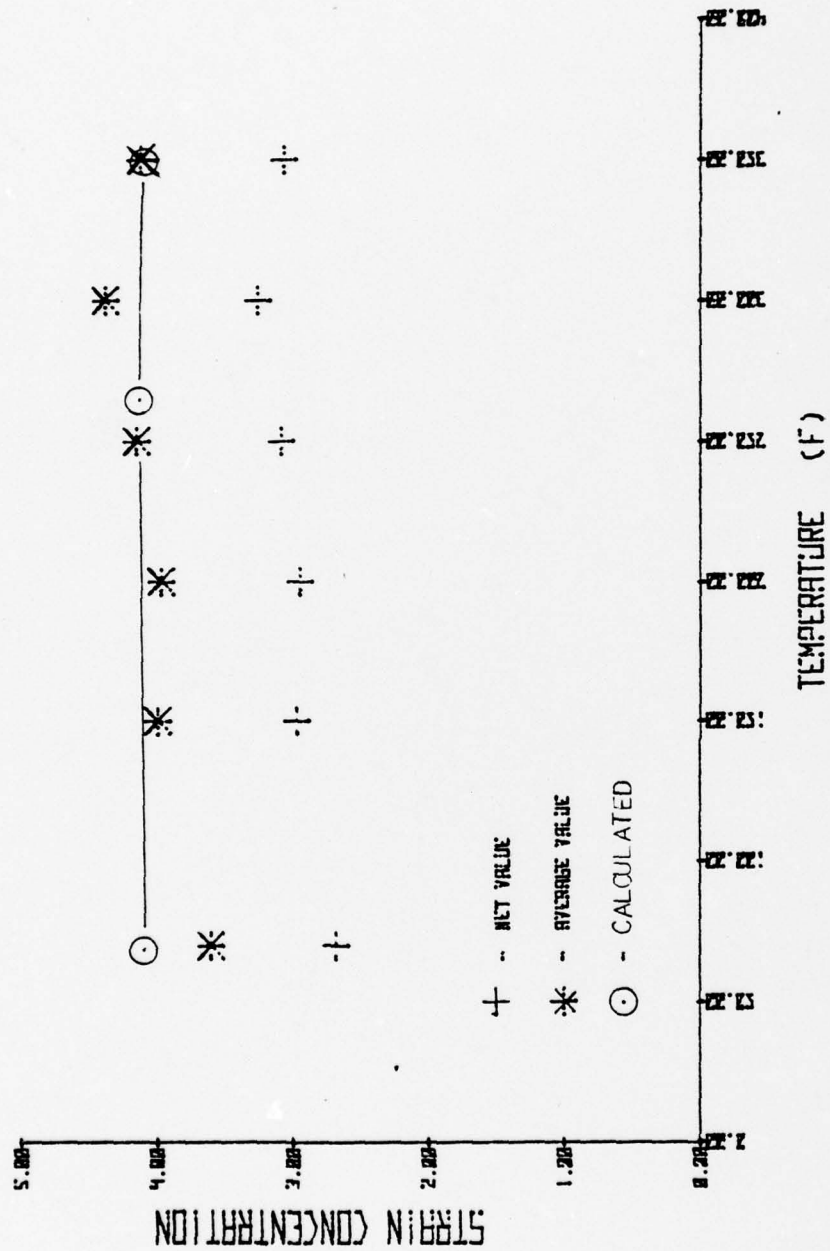


Figure 21. Specimen 208, K vs. Temperature.

BEST AVAILABLE COPY

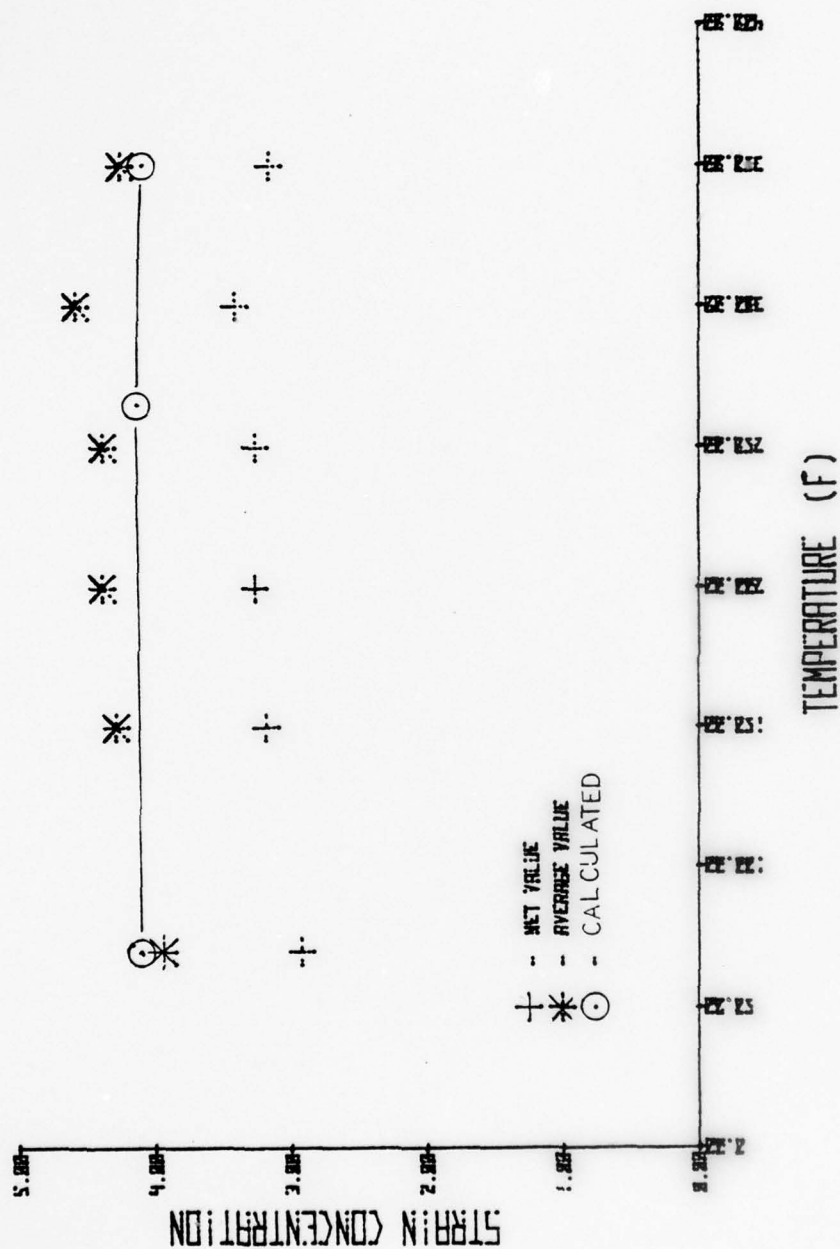


Figure 22. Specimen 305, K vs. Temperature.

shows a predicted change in the strain concentration factor, but only a 0.75% change. The actual strain concentration values are shown to increase by approximately 20% at 300 degrees Fahrenheit over the room temperature values.

V. CONCLUSIONS AND RECOMMENDATIONS

The work reported here shows that stress concentration factors in $[0/\pm 45/0]_s$ graphite/epoxy composites are temperature dependent. Values of K_{total} are 20% higher at 300 degrees Fahrenheit than at room temperature. This variation is not predicted by classical solutions for homogeneous orthotropic plates with holes, even when temperature dependence of elastic moduli is considered.

Stress concentration factors for the $[0/\pm 45/0]_s$ graphite/epoxy composites tested are lower at room temperature than values predicted by classical solutions. This conclusion agrees with previous work [13].

The ultimate strength of flat plate tensile specimens in this study did not vary appreciably in testing from room temperature to 350 degrees Fahrenheit.

It is recommended that further testing of the effects of temperature variation on stress concentration factors be undertaken, including the effects of different stacking sequences.

Testing of composite plates with holes under off-axis tensile loading should also be undertaken, to determine what stress concentration effects are produced at elevated temperatures.

Further testing should also include the effects of changes in strain rate on the strain concentration factor.

APPENDIX A

K_T CALCULATION: PHOTOELASTIC SPECIMEN

Calculation of strain concentration factor (predicted) for photoelastic specimen: two layers of PS-1C photoelastic plastic, one layer of $[0/\pm 45/0]_s$ graphite/epoxy composite.

1. For the G/E composite, measured elastic constants were:

$$E_1 = 11.51 \text{ E6 lb/in}^2$$

$$E_2 = 2.58 \text{ E6 lb/in}^2$$

$$\nu_{12} = 0.76$$

$$\nu_{21} = 0.17$$

$$G_{12} = 3.64 \text{ E6 lb/in}^2$$

The stiffness matrix for this orthotropic material in plane stress, then, is:

$$[Q] = \begin{bmatrix} Q_{11} & Q_{12} & 0 \\ Q_{12} & Q_{22} & 0 \\ 0 & 0 & Q_{66} \end{bmatrix}$$

where the Q_{ij} 's are calculated using Jones [9] formulas 2.61:

$$Q_{11}^C = \frac{E_1}{1 - \nu_{21}\nu_{12}} = 13.217 \text{ E6 lb/in}^2$$

$$Q_{12}^C = \frac{\nu_{21}E_1}{1 - \nu_{21}\nu_{12}} = 2.247 \text{ E6 lb/in}^2$$

$$Q_{22}^C = \frac{E_2}{1 - \nu_{21}\nu_{12}} = 2.963 \text{ E6 lb/in}^2$$

$$Q_{66}^C = G_{12} = 3.64 \text{ E6 lb/in}^2$$

Graphite/epoxy thickness was $t^C = 0.040$ inches.

2. For the photoelastic material, the manufacturer lists the elastic constants as:

$$E^P = 0.462 \text{ E6 lb/in}^2$$

$$\nu^P = 0.36$$

and, for an isotropic material,

$$G^P = \frac{E}{2(1 + \nu)} = 0.170$$

The stiffness matrix for this isotropic material has the same form as that in part 1 above, but the Q_{ij}^P are calculated using Jones [9] formulas 2.66:

$$Q_{11}^P = Q_{22}^P = \frac{E^P}{1 - \nu^2} = 0.531 \text{ E6 lb/in}^2$$

$$Q_{12}^P = \frac{\nu E^P}{1 - \nu^2} = 0.191 \text{ E6 lb/in}^2$$

$$Q_{66}^P = G^P = 0.170 \text{ E6 lb/in}^2$$

Each photoelastic layer had thickness $t^P = 0.042$ inches.

3. The apparent stiffnesses for the specimen, then, are found by summing through the thickness of the specimen and dividing by the total thickness; i.e.,

$$Q_{ij}^T = \frac{1}{t} \sum Q_{ij} \Delta t =$$

$$= \frac{1}{t^C + 2t^P} [t^C Q_{ij}^C + 2t^P Q_{ij}^P] =$$

$$= \frac{1}{0.124 \text{ in}} [(0.040 \text{ in}) Q_{ij}^C + (0.084 \text{ in}) Q_{ij}^P]$$

$$Q_{11}^T = 4.623 \text{ E6 lb/in}^2$$

$$Q_{12}^T = 0.854 \text{ E6 lb/in}^2$$

$$Q_{22}^T = 1.315 \text{ E6 lb/in}^2$$

$$Q_{66}^T = 1.289 \text{ E6 lb/in}^2$$

4. The apparent engineering constants for the specimen may be found by solving the equations used in part 1 for the desired constants. The results are:

$$E_1^T = Q_{11}^T - \frac{(Q_{12}^T)^2}{Q_{22}^T} = 4.068 \text{ E6 lb/in}^2$$

$$E_2^T = Q_{22}^T - \frac{(Q_{12}^T)^2}{Q_{11}^T} = 1.157 \text{ E6 lb/in}^2$$

$$\nu_{12}^T = \frac{Q_{12}^T}{Q_2^T} = 0.649$$

$$\nu_{21}^T = \frac{Q_{12}^T}{Q_1^T} = 0.185$$

$$G_{12}^T = Q_{66}^T = 1.289 \text{ E6 lb/in}^2$$

5. Finally, when these engineering constants are used in Lekhnitskii's [3] strain concentration solution:

$$n = \sqrt{2\left(\frac{E_1}{E_2} - 12\right) + \frac{E_1}{G_{12}}} = 2.98$$

$$K = 1 + n = 3.98$$

APPENDIX B

K_T CALCULATION: GRAPHITE/EPOXY LAMINATE

Calculation of strain concentration factor (predicted) in a $[0/\pm 45/0]_s$ graphite/epoxy laminate at elevated temperatures:

1. Engineering constants for a G/E lamina were extracted from handbook data [8]. For a sample calculation at 350 degrees F use

$$E_1 = 28.5 \text{ E6 lb/in}^2$$

$$E_2 = 1.78 \text{ E6 lb/in}^2$$

$$G_{12} = .87 \text{ E6 lb/in}^2$$

$$\nu_{12} = .31$$

ν_{12} can be calculated from

$$E_1 \nu_{21} = E_2 \nu_{12}$$

The stiffness matrix for this lamina in plane stress is

$$[Q] = \begin{bmatrix} Q_{11} & Q_{12} & 0 \\ Q_{12} & Q_{22} & 0 \\ 0 & 0 & Q_{66} \end{bmatrix}$$

where the Q_{ij} 's are calculated using Jones [9] formulas 2.61:

$$Q_{11} = \frac{E_1}{1 - \nu_{12}\nu_{21}} = 28.67 \text{ E6 lb/in}^2$$

$$Q_{12} = \frac{\nu_{12} E_2}{1 - \nu_{12} \nu_{21}} = 0.56 \text{ E6 lb/in}^2$$

$$Q_{22} = \frac{E_2}{1 - \nu_{12} \nu_{21}} = 1.79 \text{ E6 lb/in}^2$$

$$Q_{66} = G_{12} = .87 \text{ E6 lb/in}^2$$

2. To find the laminate stiffness constants classical laminate theory is used. Transformation equations, [T], from elementary mechanics are used to express stresses in a X - Y coordinate system in terms of stresses in a 1 - 2 coordinate system where

$$[T] = \begin{bmatrix} \cos^2 \theta & \sin^2 \theta & 2 \sin \theta \cos \theta \\ \sin^2 \theta & \cos^2 \theta & -2 \sin \theta \cos \theta \\ -\sin \theta \cos \theta & \sin \theta \cos \theta & \cos^2 \theta - \sin^2 \theta \end{bmatrix}$$

and a transformed reduced stiffness matrix, $[\bar{Q}]$, is defined as

$$[\bar{Q}] = [T] [Q] [T]^T$$

In terms of reduced stiffness coefficients, Q_{ij} , the transformed reduced stiffness coefficients are

$$\bar{Q}_{11} = Q_{11} \cos^4 \theta + 2(Q_{12} + 2Q_{66}) \sin^2 \theta \cos^2 \theta + Q_{22} \sin^4 \theta$$

$$\bar{Q}_{12} = (Q_{11} + Q_{22} - 4Q_{66}) \sin^2 \theta \cos^2 \theta + Q_{12} (\sin^4 \theta + \cos^4 \theta)$$

$$\bar{Q}_{22} = Q_{11} \sin^4 \theta + 2(Q_{12} + 2Q_{66}) \sin^2 \theta \cos^2 \theta + Q_{22} \cos^4 \theta$$

$$\begin{aligned} \bar{Q}_{16} = & -(Q_{11} - Q_{12} - 2Q_{66}) \sin \theta \cos^3 \theta - (Q_{12} - Q_{22} + \\ & + 2Q_{66}) \sin^3 \theta \cos \theta \end{aligned}$$

$$\bar{Q}_{26} = -(Q_{11} - Q_{12} - 2Q_{66})\sin^3\theta\cos\theta - (Q_{12} - Q_{22} + 2Q_{66})\sin\theta\cos^3\theta$$

$$\bar{Q}_{66} = (Q_{11} + Q_{22} - 2Q_{12} - 2Q_{66})\sin^2\theta\cos^2\theta + Q_{66}(\sin^4\theta + \cos^4\theta)$$

For $\theta = 0$ degrees

$$\bar{Q}_{11} = Q_{11} = 28.67 \text{ E6 lb/in}^2$$

$$\bar{Q}_{12} = Q_{12} = .56 \text{ E6 lb/in}^2$$

$$\bar{Q}_{22} = Q_{22} = 1.79 \text{ E6 lb/in}^2$$

$$\bar{Q}_{16} = Q_{16} = 0.0$$

$$\bar{Q}_{26} = Q_{26} = 0.0$$

$$\bar{Q}_{66} = Q_{66} = .86 \text{ E6 lb/in}^2$$

For $\theta = 45$ degrees

$$\bar{Q}_{11} = 8.765 \text{ E6 lb/in}^2$$

$$\bar{Q}_{12} = 7.025 \text{ E6 lb/in}^2$$

$$\bar{Q}_{22} = 8.765 \text{ E6 lb/in}^2$$

$$\bar{Q}_{16} = 6.720 \text{ E6 lb/in}^2$$

$$\bar{Q}_{26} = 6.720 \text{ E6 lb/in}^2$$

$$\bar{Q}_{66} = 7.335 \text{ lb/in}^2$$

For $\theta = -45$ degrees

$$\bar{Q}_{11} = 8.765 \text{ E6 lb/in}^2$$

$$\bar{Q}_{12} = 7.025 \text{ E6 lb/in}^2$$

$$\bar{Q}_{22} = 8.765 \text{ E6 lb/in}^2$$

$$\bar{Q}_{16} = -6.720 \text{ E6 lb/in}^2$$

$$\bar{Q}_{26} = -6.720 \text{ E6 lb/in}^2$$

$$\bar{Q}_{66} = 7.335 \text{ E6 lb/in}^2$$

3. Realizing that symmetric laminates have no coupling between bending and extension, in-plane forces will produce extension only or

$$\{N_x\} = [A] \{\epsilon_x^0\}$$

where N_x 's are in plane forces, A_{ij} 's are the extensional stiffnesses and ϵ_x^0 's are the middle surface strains. From Jones [9] for an orthotropic laminate

$$A_{ij} = \sum_{k=1}^n (\bar{Q}_{ij}) t_k$$

where t_k is the thickness of a lamina. Noting that the thickness of each lamina are the same

$$[\bar{Q}_{ij}]^C = \frac{\sum \bar{Q}_{ij}}{n}$$

where n is the number of lamina. In this case the laminate stiffness constants are:

$$\bar{Q}_{11}^C = 18.7175 \text{ E6 lb/in}^2$$

$$\bar{Q}_{12}^C = 3.7925 \text{ E6 lb/in}^2$$

$$\bar{Q}_{22}^C = 5.2775 \text{ E6 lb/in}^2$$

$$\bar{Q}_{16}^C = 0.0$$

$$\bar{Q}_{26}^C = 0.0$$

$$\bar{Q}_{66}^C = 4.1025 \text{ E6 lb/in}^2$$

4. The equivalent engineering constants for the laminate can now be found from

$$\bar{Q}_{11}^C = \frac{E_1}{1 - \nu_{12}\nu_{21}}$$

$$\bar{Q}_{12}^C = \frac{\nu_{12}E_2}{1 - \nu_{12}\nu_{21}}$$

$$\bar{Q}_{22}^C = \frac{E_2}{1 - \nu_{12}\nu_{21}}$$

$$\bar{Q}_{66}^C = G_{12}$$

Simplifying produces the equivalent composite engineering constants which are

$$E_1^C = 15.99 \text{ E6 lb/in}^2$$

$$E_2^C = 4.51 \text{ E6 lb/in}^2$$

$$G_{12}^C = 4.1025 \text{ E6 lb/in}^2$$

$$\nu_{12}^C = .719$$

$$\nu_{21}^C = .203$$

5. Finally, when these engineering constants are used in Lekhnitskii's [3] strain concentration solution,

$$n = \sqrt{2 \left(\frac{E_1^C}{E_2^C} - \nu_{12}^C \right) + \frac{E_1^C}{G_{12}^C}} = 3.09$$

$$K = (1 + n) = 4.09$$

APPENDIX C
PHOTOELASTIC DATA

Stress Concentration Data 25 February 1977

Plate # 001 y-Direction

of Runs: 1 Load 750.0 F = 38.298

<u>Y/R</u>	<u>TNN</u>	<u>TNO</u>	<u>NN</u>	<u>NO</u>	<u>EPSX</u>	<u>EPSY</u>	<u>K</u>
FF	-2.5	-3.0	18.5	21.5	603	-201	1.00
1.0	-5.5	-3.0	63.5	*****	1943	*****	3.22
1.3	-2.5	-3.0	29.5	37.5	1101	-124	1.83
1.7	-2.5	-3.0	21.5	24.0	631	-287	1.05
2.0	-2.5	-3.0	20.5	23.8	658	-222	1.09
2.3	-2.5	-3.0	19.6	23.5	675	-170	1.12
2.7	-2.5	-3.0	19.6	21.8	578	-268	0.96
3.0	-2.5	-3.0	19.6	21.5	561	-285	0.93
3.3	-6.0	-3.0	13.3	*****	543	*****	0.90

APPENDIX D

TENSILE TESTS

GAGE	STRAIN (microinch/inch) - at 70 degrees F - σ (ksi) of:																E (msi)	ν
	3.08	6.16	9.24	12.32	15.39	18.47	21.55	24.64	27.71	30.79	33.87	36.95						
106	310	550	810	1050	1330	1620	1850	2105	2340	2600	2845	3130					11.7	
106	310	555	810	1060	1330	1580	1850	2100	2355	2600	2860	3140					11.7	
107	280	500	760	1000	1270	1510	1780	2020	2275	2575	2790	3060					12.1	
107	280	500	730	980	1250	1490	1750	1990	2230	2470	2720	3000					12.4	
107	220	530	780	1030	1310	1540	1830	2100	2340	2600	2850	3110					11.9	
107	300	530	770	1025	1280	1520	1800	2040	2290	2540	2775	3040					12.1	
107	330	550	810	1050	1290	1540	1750	2050	2290	2520	2770	3020					12.0	
107	320	550	800	1040	1290	1530	1750	2030	2260	2510	2760	3010					12.1	
107	320	560	810	1050	1250	1540	1750	2040	2290	2530	2770	3030					12.0	
204	270	500	740	970	1230	1480	1700	1980	2200	2450	2690	2930					12.5	
	-160	-280	-430	-575	-740	-880	-1010	-1180	-1325	-1480	-1740	-1790					.61	
205	290	530	760	1000	1240	1485	1740	1990	2220	2480	2700	2970					12.4	
	-160	-325	-465	-620	-770	-935	-1110	-1275	-1425	-1590	-1745	-1920					.64	
301	300	555	810	1060	1340	1600	1855	2130	2380	2625	2890	3175					11.6	
	-175	-325	-460	-600	-780	-925	-1060	-1220	-1360	-1505	-1660	-1825					.57	
302	310	575	850	1160	1415	1675	1945	2210	2480	2730	2970	3250					11.1	
	-125	-240	-370	-495	-630	-760	-900	-1040	-1170	-1300	-1440	-1590					.47	
206	325	565	840	1095	1360	1625	1905	2175	2425	2705	2940	3220					11.4	
	-180	-320	-460	-630	-770	-915	-1080	-1225	-1370	-1545	-1705	-1820					.57	
207	320	605	820	1060	1340	1570	1845	2090	2345	2620	2860	3140					11.7	
	-180	-320	-420	-605	-750	-890	-1030	-1170	-1300	-1440	-1580	-1710					.55	
303	315	540	800	1040	1300	1660	1810	2045	2280	2510	2760	3050					11.9	
	-160	-280	-420	-545	-685	-845	-970	-1115	-1250	-1400	-1550	-1740					.54	
304	320	550	805	1050	1325	1575	1830	2065	2305	2550	2790	3030					11.9	
	-140	-225	-380	-525	-650	-790	-930	-1075	-1200	-1355	-1490	-1625					.52	
																avg	11.9	.56

GAGE	STRAIN (microinch/inch) - at 150 degrees F - σ (ksi) of:												E(msi)	ν	HEAT SOAKED	
	3.08	6.16	9.24	12.32	15.39	18.47	21.55	24.64	27.71	30.79	33.87	36.95				
107	175	400	660	900	1150	1410	1675	1900	2150	2420	2660	2910	13.0			NO
107	275	490	740	980	1240	1420	1720	1960	2150	2410	2650	2880	12.7			NO
107	310	530	750	980	1220	1400	1640	1870	2090	2320	2525	2750	13.1			NO
204	270	500	740	960	1220	1460	1710	1950	2175	2390	2630	2900	12.8			NO
	-175	-330	-475	-625	-780	-950	-1115	-1270	-1430	-1565	-1715	-1900		.65		
205	250	460	670	870	1065	1260	1460	1670	1840	2040	2210	2420	14.8			NO
	-180	-330	-480	-630	-790	-940	-1100	-1240	-1375	-1530	-1670	-1820		.75		
301	220	455	675	920	1125	1340	1555	1805	1990	2210	2370	2600	13.9			NO
	-140	-240	-405	-540	-700	-825	-970	-1110	-1230	-1370	-1490	-1610		.62		
302	300	605	820	1180	1340	1575	1840	2080	2335	2550	2740	3020	11.8			NO
	-160	-305	-445	-680	-740	-880	-1050	-1200	-1390	-1425	-1610	-1750		.57		
302	275	570	780	1100	1400	1650	1940	2200	2460	2730	3005	3300	11.2			YES
	-165	-300	-450	-590	-750	-905	-1080	-1225	-1380	-1500	-1660	-1825		.55		
avg													13.1			NO
avg													11.2			YES

GAGE	STRAIN (microinch/inch) - at 200 degrees F - σ (ksi) of:												E(msi)	ν	HEAT SOAKED
	3.08	6.16	9.24	12.32	15.39	18.47	21.55	24.64	27.71	30.79	33.87	36.95			
204	100	160	210	275	320	380	455	530	580	645	700	770	46.9	.73	NO
	- 70	- 125	- 155	- 200	- 250	- 290	- 345	- 375	- 425	- 460	- 510	- 550			
205	70	125	160	200	230	275	315	360	390	430	460	500	68.3	.83	NO
	- 50	- 80	- 120	- 155	- 200	- 230	- 260	- 300	- 330	- 365	- 400	- 430			
301	55	105	150	195	235	300	340	380	425	455	480	525	65.9	.64	NO
	- 55	- 80	- 110	- 140	- 160	- 180	- 200	- 230	- 265	- 285	- 305	- 340			
301	300	530	750	980	1200	1415	1630	1880	2100	2310	2510	2750	13.1	.69	YES
	- 200	- 340	- 500	- 675	- 840	- 980	- 1135	- 1280	- 1440	- 1580	- 1730	- 1930			
302	135	200	260	330	400	460	550	600	650	715	760	820	40.9	.50	NO
	- 40	- 80	- 130	- 165	- 190	- 230	- 275	- 305	- 345	- 370	- 400	- 425			
206	50	100	145	190	225	270	310	350	380	410	460	500	70.9	.82	NO
	- 50	- 90	- 130	- 150	- 190	- 220	- 250	- 280	- 310	- 340	- 370	- 415			
	avg 58.6												58.6	.70	NO
	avg 13.1												13.1	.69	YES

GAGE	STRAIN (microinch/inch) - at 250 degrees F - σ (ksi) of:												E (msi)	ν	HEAT SOAKED
	3.08	6.16	9.24	12.32	15.38	18.47	21.55	24.64	27.71	30.79	33.87	36.95			
107	170	310	470	610	770	910	1060	1180	1320	1470	1610	1740	20.7		YES
107	110	230	320	400	510	590	690	810	900	1020	1170	1275	29.9		YES
107	140	260	370	500	630	710	840	940	1060	1160	1240	1370	26.1		YES
107	110	220	310	430	550	680	790	960	1045	1140	1220	1330	27.3		YES
107	170	310	450	570	740	880	1020	1140	1290	1430	1560	1690	21.3		YES
204	100	140	170	225	265	325	360	415	455	520	555	620	57.9		NO
	- 45	- 90	-120	-150	-180	-205	- 240	- 270	- 300	- 330	- 360	- 405	.65		
205	65	100	150	170	250	290	315	350	385	420	450	500	69.7		NO
	- 40	- 70	-100	-130	-150	-175	- 220	- 250	- 280	- 320	- 355	- 390	.72		
205	100	160	240	330	380	435	510	565	650	725	780	830	42.1		YES
	- 55	-125	-180	-230	-300	-355	- 410	- 470	- 520	- 570	- 625	- 690	.79		
301	35	105	140	180	215	250	300	340	370	385	410	455	75.4		NO
	- 35	- 80	-115	-140	-155	-180	- 205	- 220	- 250	- 285	- 305	- 325	.72		
302	75	120	175	225	270	315	370	415	450	500	550	600	59.1		NO
	- 45	- 70	- 95	-125	-150	-180	- 230	- 265	- 290	- 310	- 340	- 355	.60		
207	65	140	180	220	270	320	375	425	470	520	560	605	57.9		NO
	- 25	-110	-140	-170	-180	-220	- 240	- 250	- 275	- 295	- 330	- 370	.63		
	avg												64.0	.66	NO
	avg												27.9	.79	YES

GAGE	STRAIN (microinch/inch) - at 300 degrees F - σ (ksi) of:												E(msi)	ν	HEAT SOAKED
	3.08	6.16	9.24	12.32	15.38	18.47	21.55	24.64	27.71	30.79	33.87	36.95			
204	40	75	115	150	200	240	280	345	400	470	505	555	7.12		NO
	- 35	- 65	- 100	- 140	- 170	- 200	- 250	- 260	- 280	- 340	- 375	- 435		.79	
204	145	200	260	315	365	430	520	610	670	750	815	890	40.2		YES
	- 40	- 75	- 125	- 180	- 225	- 275	- 315	- 370	- 410	- 445	- 495	- 540		.59	
205	60	125	170	205	245	265	310	345	385	425	475	520	68.0		NO
	- 45	- 60	- 100	- 140	- 180	- 210	- 245	- 270	- 300	- 340	- 370	- 400		.75	
301	75	90	130	165	200	235	270	315	355	400	445	500	75.5		NO
	- 30	- 50	- 80	- 100	- 140	- 155	- 180	- 210	- 245	- 270	- 270	- 300		.64	
302	50	90	140	200	245	300	360	415	460	515	565	610	60.8		NO
	- 40	- 70	- 100	- 125	- 150	- 180	- 200	- 230	- 260	- 280	- 315	- 365		.59	
303	50	110	180	225	265	320	355	400	445	500	540	580	60.5		NO
	- 25	- 50	- 80	- 100	- 125	- 145	- 175	- 190	- 235	- 270	- 300	- 335		.51	
													avg	67.2	NO
													avg	40.2	YES

GAGE	STRAIN (microinch/inch) - at 350 degrees F - σ (ksi) of:												E(msi)	ν	HEAT SOAKED
	3.08	6.16	9.24	12.32	15.39	18.47	21.55	24.64	27.71	30.79	33.87	36.95			
106	170	275	350	520	645	770	890	1000	1110	1245	1360	1470	24.5		YES
107	220	350	480	580	690	770	900	1020	1150	1250	1350	1480	23.5		YES
107	130	260	375	470	570	700	830	920	1050	1170	1280	1380	26.3		YES
204	70	130	200	255	320	380	445	500	560	645	700	790	48.1		NO
	- 50	- 80	- 125	- 160	- 200	- 230	- 265	- 300	- 320	- 360	- 385	- 430		.58	
205	70	135	200	250	290	370	420	455	500	570	590	650	53.4		NO
	- 40	- 80	- 105	- 145	- 190	- 225	- 280	- 330	- 370	- 410	- 460	- 500		.70	
301	45	80	140	175	205	265	305	355	390	430	475	510	71.2		NO
	- 50	- 80	- 125	- 150	- 180	- 180	- 205	- 260	- 300	- 330	- 355	- 395		.77	
302	50	110	200	250	320	370	425	475	525	560	625	700	52.1		NO
	- 30	- 75	- 120	- 155	- 170	- 200	- 240	- 265	- 300	- 315	- 380	- 405		.58	
304	70	135	175	250	275	340	375	425	475	525	575	600	56.9		NO
	- 25	- 30	- 40	- 80	- 120	- 160	- 170	- 200	- 225	- 255	- 280	- 290		.44	
													avg	56.3	NO
													avg	24.8	YES

APPENDIX E

ULTIMATE STRENGTH DATA

<u>SPECIMEN</u>	<u>DELAMINATED</u>	<u>GOOD BREAK</u>	<u>HEAT SOAKED</u>	<u>TEMPERATURE (F)</u>	<u>ULTIMATE STRENGTH (msi)</u>
310	NO	YES	YES	70	96
104	YES	YES	YES	70	113
105	YES	YES	YES	70	106
201	YES	YES	YES	70	104
302	NO	YES	YES	150	105
206	YES	NO	NO	200	94
301	NO	YES	YES	200	105
205	YES	NO	YES	250	97
207	YES	NO	NO	250	90
204	YES	NO	YES	300	94
303	YES	NO	NO	300	119
107	YES	NO	YES	350	92
304	YES	YES	NO	350	112

APPENDIX F

STRAIN CONCENTRATION DATA

TEMP	1.408	2.815	4.223	5.631	7.038	8.446	9.854	11.26	12.67	14.08	15.58	16.89	NET STRESS (msi)
(F)	1.047	2.095	3.142	4.189	5.236	6.289	7.331	8.378	9.425	10.47	11.52	12.57	AVERAGE STRESS (msi)

	SPECIMEN 208											
	STRAIN (microinch/inch)											
70	355	650	975	1260	1580	1860	2220	2540	2840	3165	3475	3790
150	475	740	1075	1430	1680	1960	2305	2590	2930	3200	3500	3860
200	260	620	1100	1300	1575	1900	2270	2610	2780	3110	3455	3760
250	400	625	985	1240	1600	1900	2475	2725	2910	3175	3485	4000
300	500	750	1075	1510	1700	2140	2290	2630	3020	3500	3950	4000
350	500	810	1250	1650	1710	1960	2320	2660	3060	3300	3550	3850

	SPECIMEN 305											
70	400	720	1080	1405	1750	2070	2410	2750	3070	3420	3750	4100
150	440	750	1110	1480	1790	2190	2480	2810	3125	3450	3820	4160
200	375	680	1100	1460	1780	2170	2480	2770	3140	3450	3770	4120
250	435	750	1090	1420	1710	2025	2400	2710	3040	3430	3760	4140
300	440	720	1070	1440	1790	2160	2450	2840	3360	3740	4110	4210
350	410	710	1130	1455	1800	2120	2460	2785	3180	3480	3800	4120

LIST OF REFERENCES

1. Yaffee, M. L., "Composite Aircraft Study in Final Stage," Aviation Week & Space Technology, v. 104 no. 16, p. 16-18, 19 April 1976.
2. Klass, P. J., "Advanced Weaponry Research Intensifies," Aviation Week & Space Technology, v. 103 no. 7, p. 34-39, 18 August 1975.
3. Lekhnitskii, S. G., Anisotropic Plates, p. 157-190, Gordon and Breach Science Publishers, 1968.
4. Linnander, R. J., Laboratory Development and Tensile Testing of Graphite/Glass/Epoxy Hybrid Composite Materials, M.S. Thesis, Naval Postgraduate School, Monterey, 1974.
5. Hanley, D. P., and Cross, S. L., Studies Related to the Acoustic Failure Resistance of Advanced Composites, paper presented at Twelfth National SAMPE Symposium "Advances in Structural Composites," Anaheim, California, 10-12 October 1967.
6. Ferris, R. L., Low Energy Impact Loading of Graphite-Epoxy Plates, M.S. Thesis, Naval Postgraduate School, Monterey, 1976.
7. Gilley, E., Roylance, D., and Schneider, N., Methods of Fiber and Void Measurement in Graphite/Epoxy Composites, Composite Materials Testing and Design (Third Conference), ASTM STP 546, American Society for Testing and Materials, p. 237-249, 1974.
8. Air Force Materials Laboratory Contract Report Number F33615-71-C-1362, Advanced Composite Design Guide, by Rockwell International Corporation, January 1973.
9. Jones, R. M., Mechanics of Composite Materials, p. 46-172, McGraw-Hill, 1975.
10. Photolastic, Inc., "Instruction Manual for 030 Series Reflection Polariscopes," 1974.
11. Saba, D. L., Stress Concentration Around Holes in Laminated Fibrous Composites, M.S. Thesis, Naval Postgraduate School, Monterey, 1975.
12. Micro-Measurements Tech. Note TN-128-2, Strain Gage Temperature Effects, p. 1-9, A-1, 1976.

13. Daniel, I. M., Rowlands, R. E., and Whiteside, J. B., "Effects of Material and Stacking Sequence on Behavior of Composite Plates with Holes," Experimental Mechanics, p. 1-9, January 1974.
14. Stanfield, W. C., Microprogrammable Integrated Data Acquisition System - Fatigue Life Data Application, M.S. Thesis, Naval Postgraduate School, Monterey, 1976.

INITIAL DISTRIBUTION LIST

	No. Copies
1. Defense Documentation Center Cameron Station Alexandria, VA 22314	2
2. Library, Code 0142 Naval Postgraduate School Monterey, CA 93940	2
3. Department Chairman, Code 67 Department of Aeronautics Naval Postgraduate School Monterey, CA 93940	1
4. Asst. Prof. M. H. Bank, Code 67Bt Department of Aeronautics Naval Postgraduate School Monterey, CA 93940	5
5. LCDR Rene J. Chicoine, USN U.S. Naval Test Pilot School Naval Air Station Patuxent River, MD 20670	1